# Trayectoria de tormentas

# General circulation in an aqua-planet
Perpetual Equinox

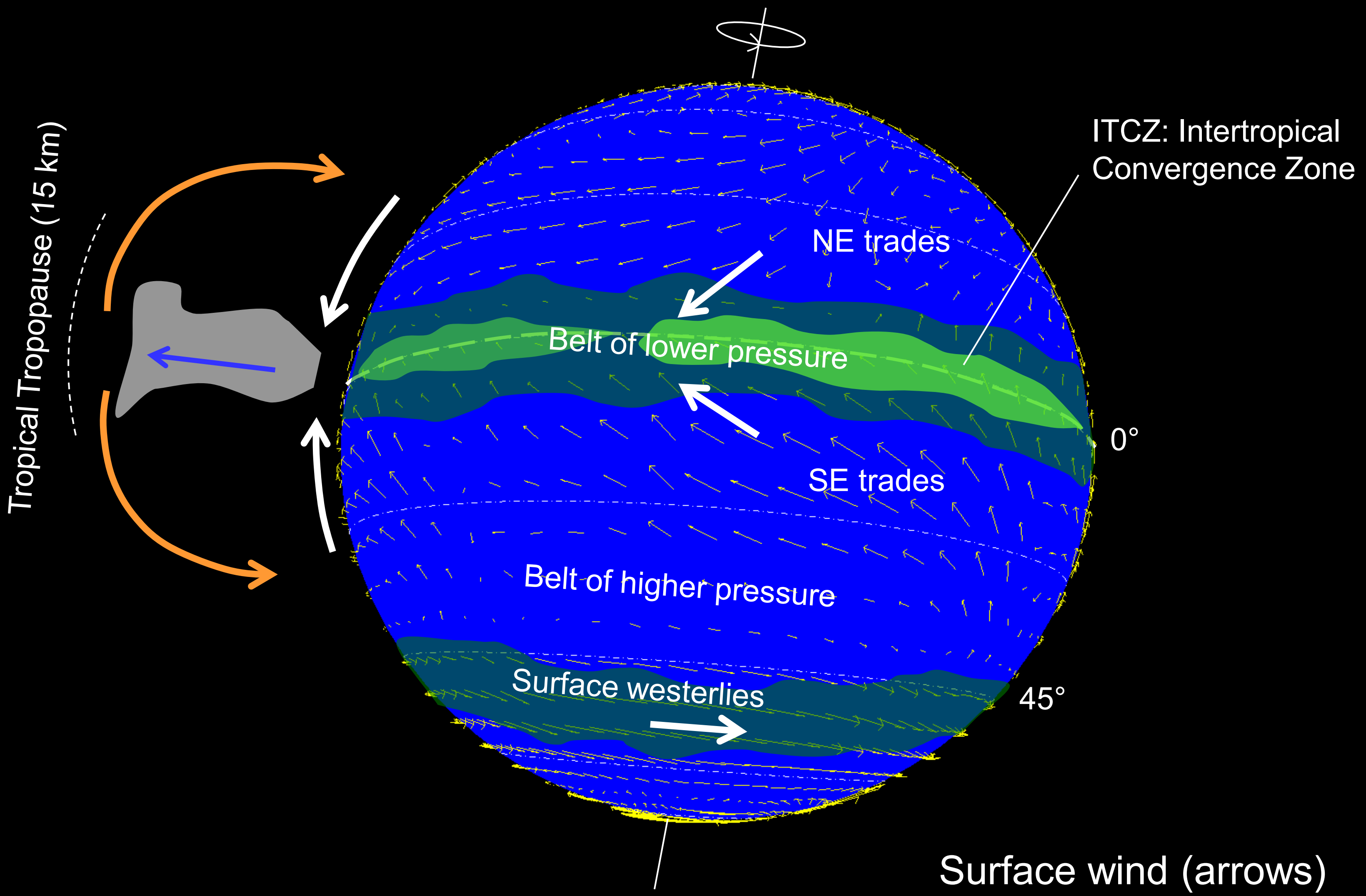


Surface wind (arrows)
Precipitation (green shadow)

# General circulation in an aqua-planet
## Perpetual Equinox

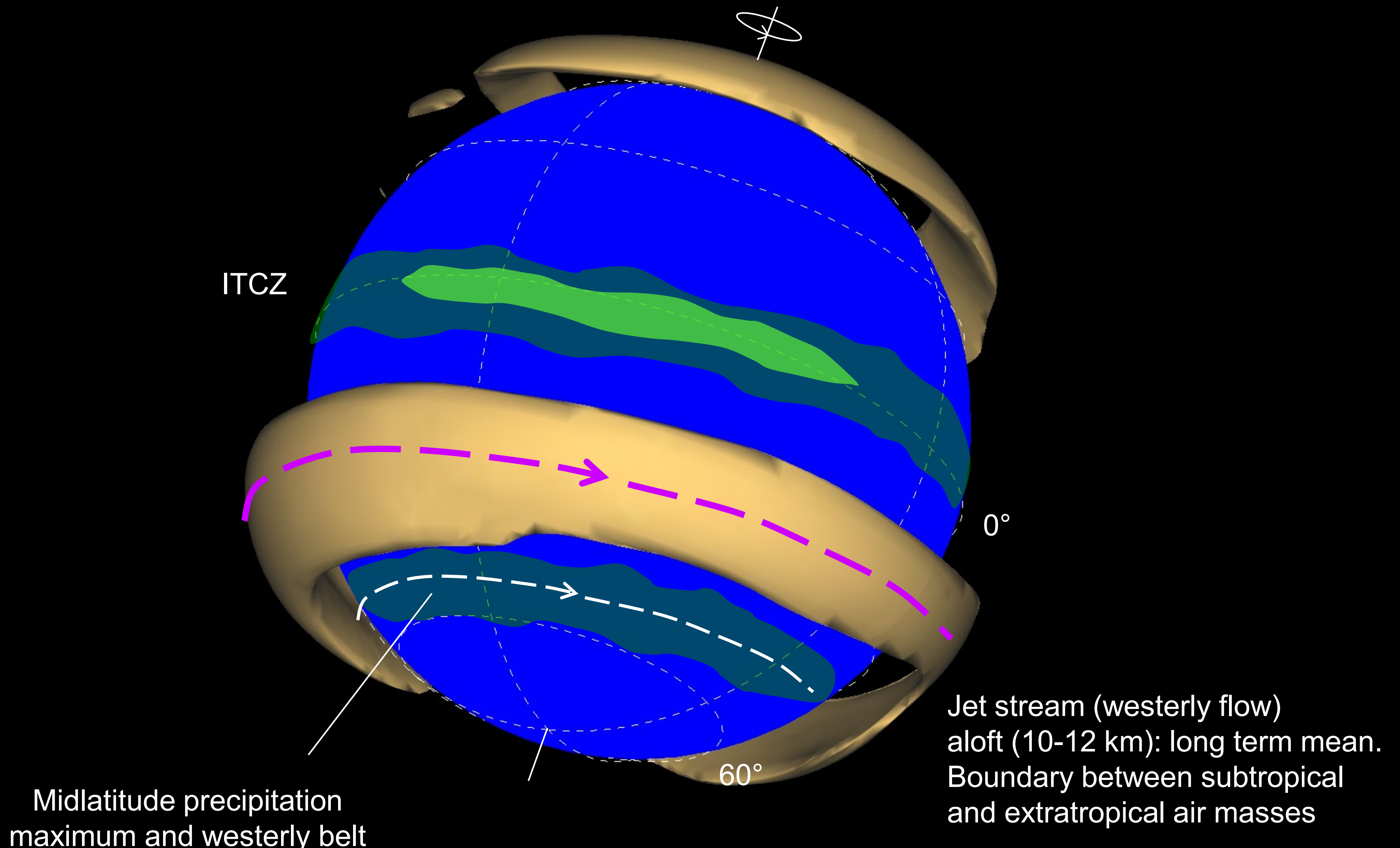

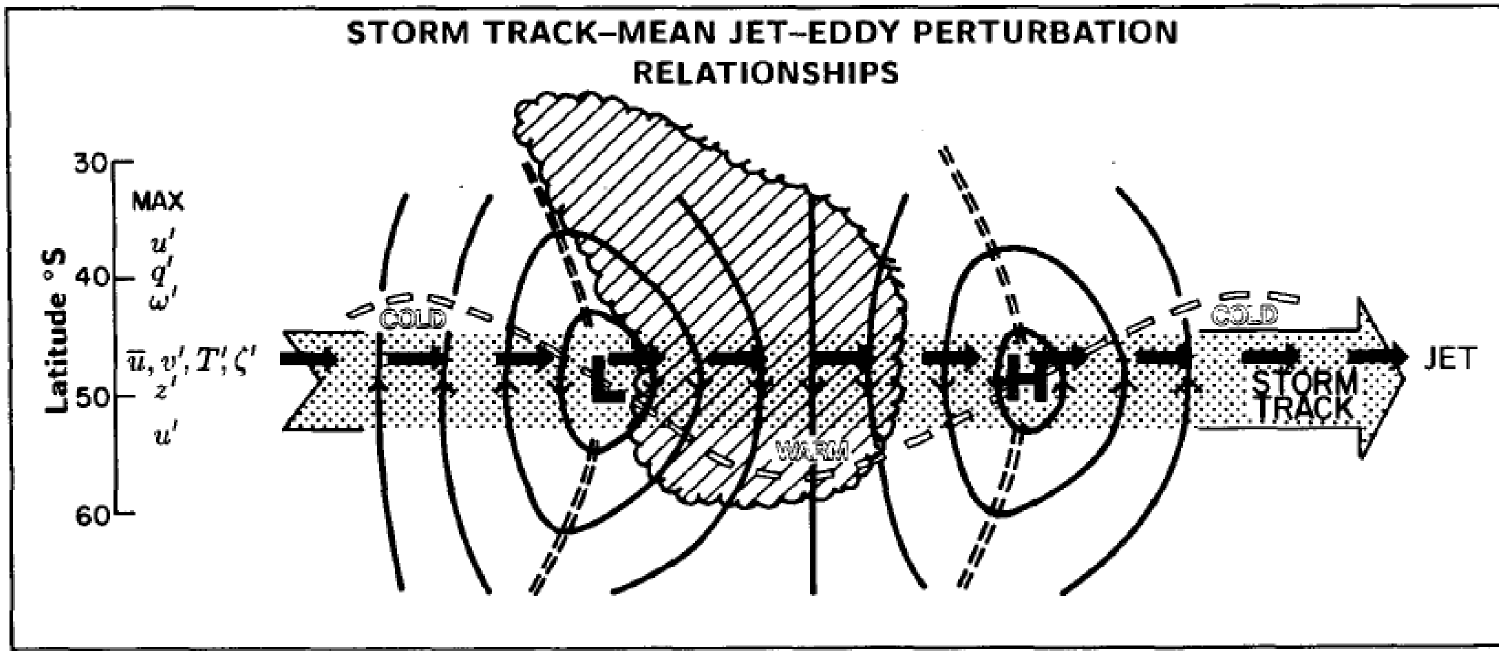


FIG. 1. Schematic plot in the SH of the relationships between the mean jet (solid heavy arrow) and storm tracks (broad stippled arrow) and associated high frequency eddy statistics. Perturbation geopotential heights are greatest in the storm track producing a maximum $\overline{z'^2}$. Maxima in all quantities are indicated at left. Vorticity perturbations are a maximum just north of the storm track owing to the Coriolis parameter variations and consistent with the geostrophic relation. Therefore, meridional wind perturbations are similarly shifted north while zonal wind perturbations are a maximum north and south of the storm track. Moreover, the perturbations are elongated north–south so that $\overline{v'^2} < \overline{u'^2}$, and they have a characteristic shape with trough and ridge lines (shown by the double line) such that there is convergence of momentum by the eddies into the storm track ($\overline{v'\zeta'} > 0$). Temperature perturbations (outlined dashed line) are a maximum in the lower troposphere and highly correlated with $-v'$. Maximum perturbations in moisture and vertical motion are closely related and occur in lower latitudes in close correspondence with $v'$ and $T'$, as indicated by the hatched cloud zone.

**Storm Tracks in the Southern Hemisphere**

Kevin E. Trenberth



Sd(z300)
High pass

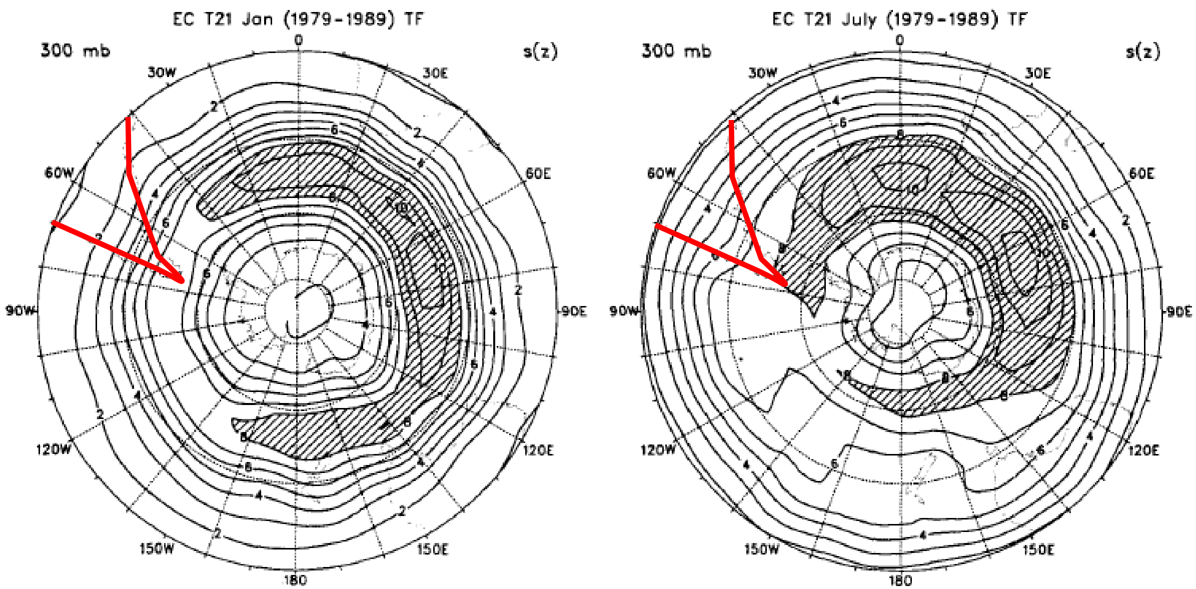


FIG. 6. Long-term 2–8-day January and July mean $s(z)$ at 300 mb in dam showing location of storm track. Values greater than 8 dam are hatched.

Sd(v300)
High pass

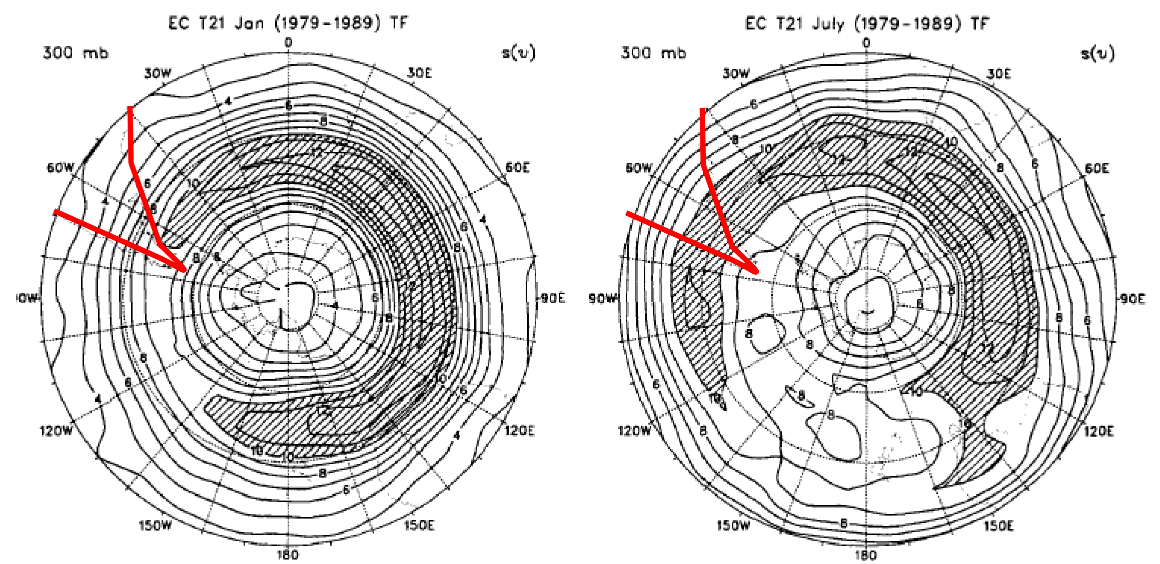


FIG. 7. Long-term 2–8-day January and July mean $s(v)$ at 300 mb; the contour interval is 1 m s$^{-1}$. Values greater than 10 m s$^{-1}$ are hatched.

# Mean Southern Hemisphere Extratropical Cyclone Behavior in the 40-Year NCEP–NCAR Reanalysis

IAN SIMMONDS AND KEVIN KEAY

*School of Earth Sciences, University of Melbourne, Parkville, Victoria, Australia*

(Manuscript received 16 November 1998, in final form 31 March 1999)

ABSTRACT

This paper presents a new climatology of Southern Hemisphere (SH) extratropical cyclones. This has been compiled by applying a state-of-the-art cyclone tracking scheme to the 6-hourly National Centers for Environmental Prediction–National Center for Atmospheric Research (NCEP–NCAR) global reanalyses spanning the period 1958–97. The results show there to be, on average, between 35 and 38 cyclonic systems per analysis (depending on season), with the greatest density [exceeding $6 \times 10^{-3}$ cyclones (deg lat)$^{-2}$] found south of 60°S in all seasons and in the Indian and west Pacific Oceans in autumn and winter. For the most part, there is a net *creation* of cyclones (i.e., cyclogenesis exceeds cyclolysis) north of about 50°S, and a net *destruction* to the south of this latitude. Having said this, the most active cyclogenesis takes place south of 45°S. The NCEP–NCAR reanalyses indicate that most SH cyclogenesis occurs at very high latitudes, and the axis of the maximum lies on, or to the south of, 60°S. This is in agreement with the deductions of many modern studies of SH cyclone behavior. The region is also host to even greater levels of cyclolytic activity.

The authors consider measures of the importance and influence (e.g., for eddy fluxes) of cyclonic systems. It is suggested that the "depth" of a system (the pressure difference between the center and the "edge" of a cyclone) is a relatively bias-free and useful measure of a cyclone's status and effect on the circulation. The greatest climatological depths are seen to lie at about 60°S, well to the north of the circumpolar trough and of the region of greatest cyclone density. The mean lifetime of cyclones that last at least 1 day is just over 3 days. Those that are located between 50° and 70°S (at their half-lifetime) endure, on average, almost one day longer than all other systems. The mean track length of winter systems is 2315 km, which reduces to 1946 km in summer.

The significance of the work presented here lies in a number of factors. First, the climatology has been derived from 40 yr of analysis, a period longer than any considered heretofore. Further, the (re)analyses used can be regarded as one of the best representations of the global atmosphere. The availability of these analyses at 6-hourly intervals means that the uncertainties with tracking of cyclones are greatly diminished. Finally, it has been compiled using one of the most sophisticated and reliable automatic cyclone finding and tracking schemes. This climatology of SH extratropical cyclones is arguably the most accurate and representative set yet assembled.

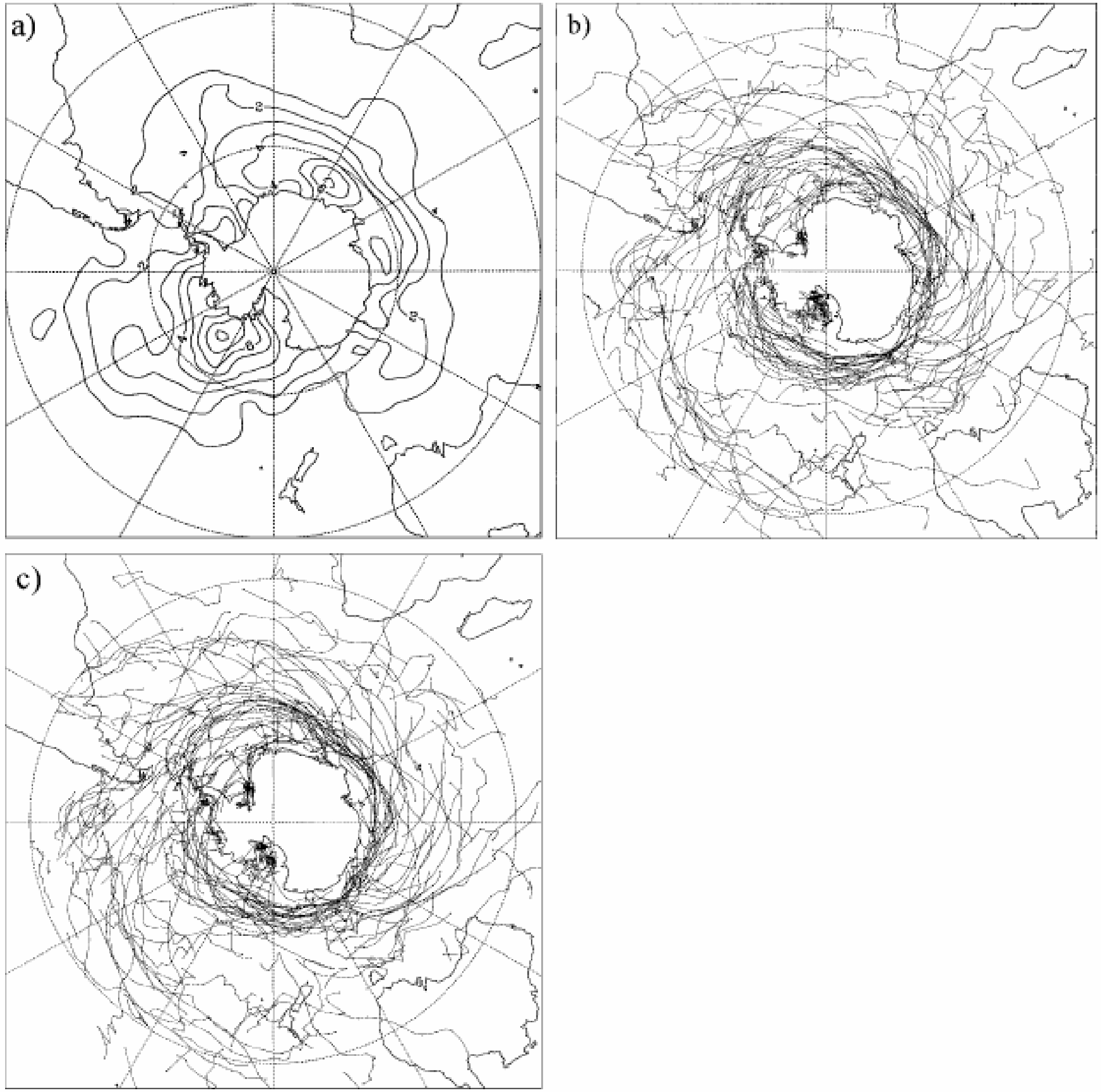


FIG. 1. (a) Temporal standard deviation of the difference between the MSLP of the initial reanalyses (I) and corrected analyses (C) for Jul 1979 (the contour interval is 1 hPa). Tracks of all SH cyclones (with a minimum lifetime of 24 h) in Jul 1979 in the (b) I and (c) C analyses.

# Todos los Ciclones

DJF

JJA



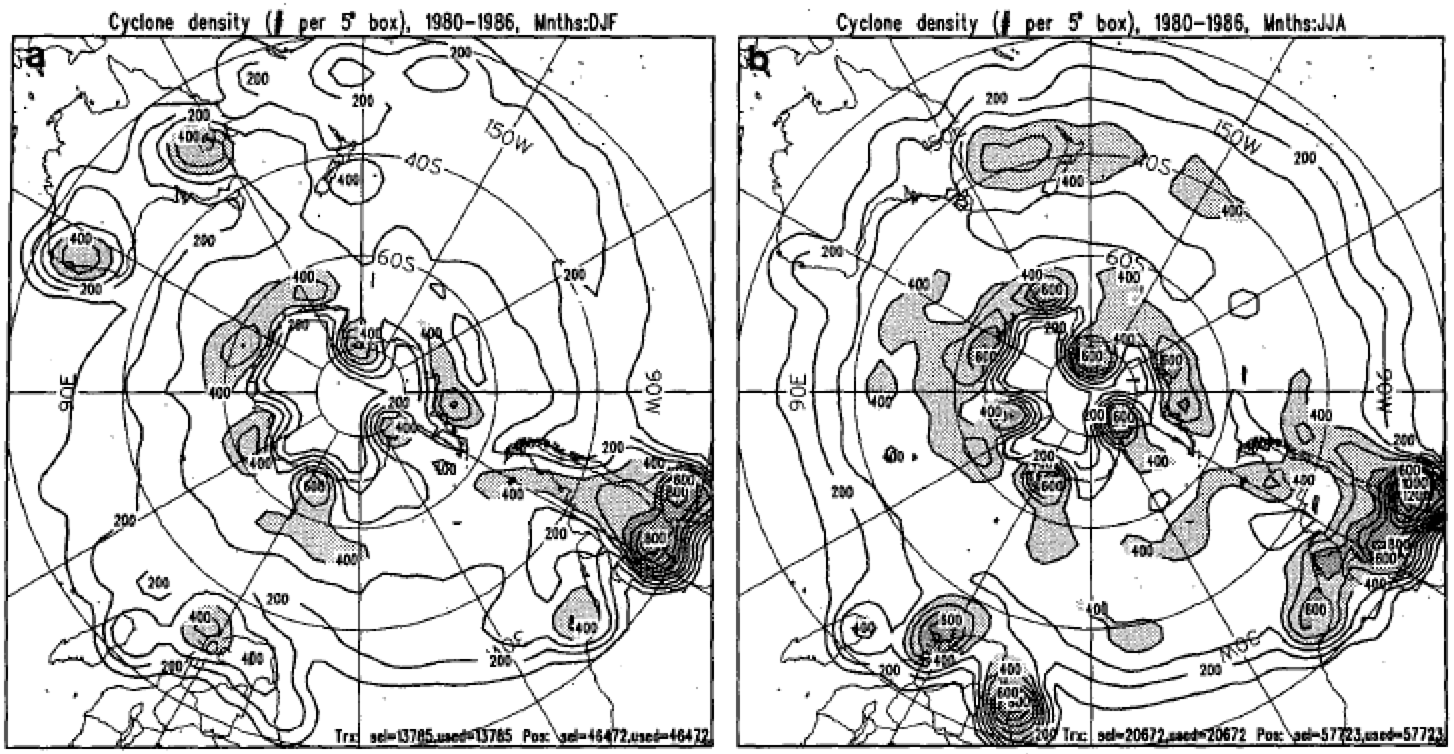


FIG. 6. Cyclone density for all cyclones for (a) December, January, and February, and (b) June, July, and August for 1980–86. Cyclones are counted as numbers of centers per 5° latitude radius circle. The contour interval is 100, with light (medium) shading for counts greater than 400 (600).

# Ciclones migratorios

DJF

JJA

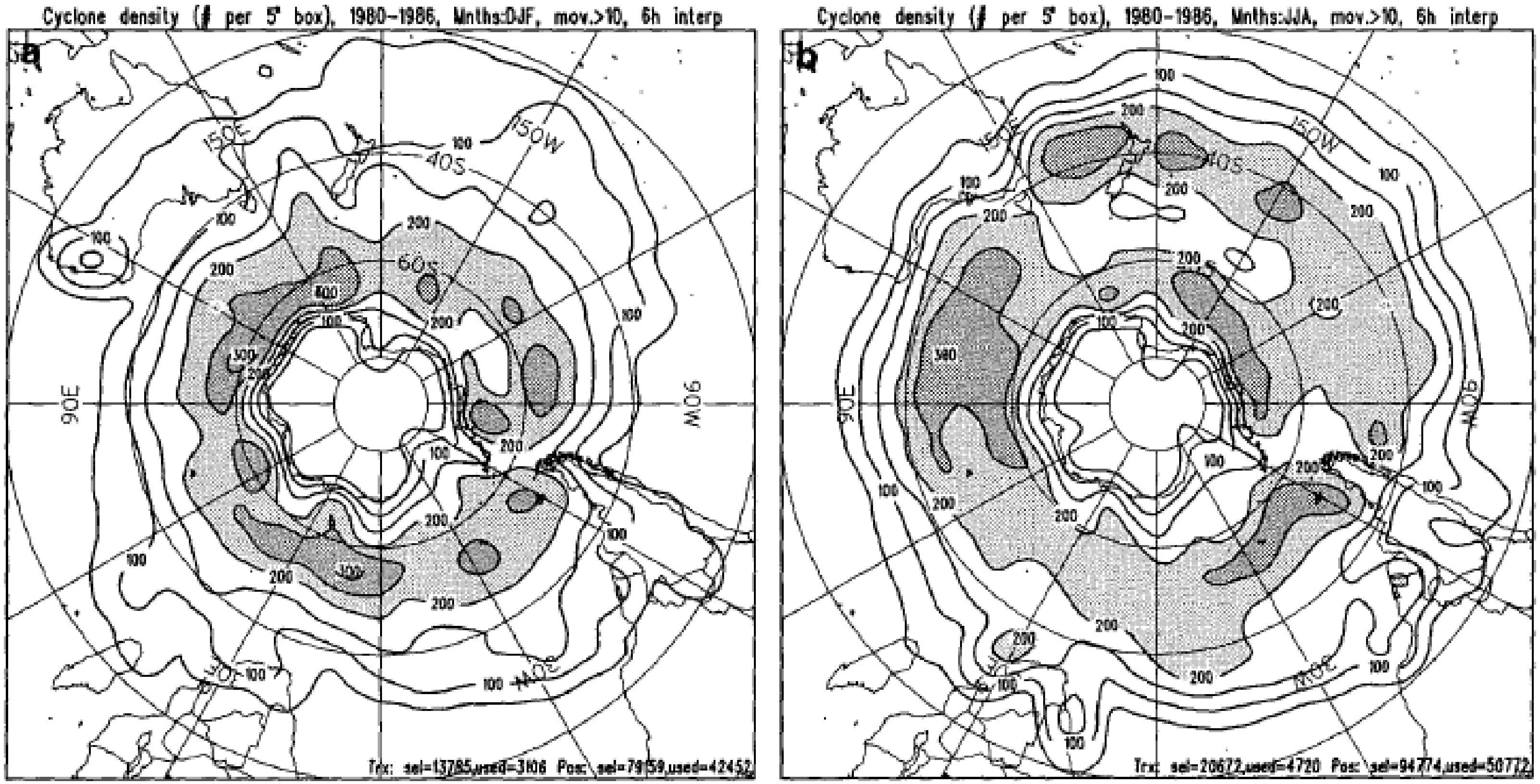


FIG. 10. As for Fig. 6 except for cyclones moving a total distance greater than 10° of latitude. Six-hour time interpolation is used. The contour interval is 50, and values greater than 200 (250) are shaded (heavily).

# Ciclones intensos

DJF

JJA

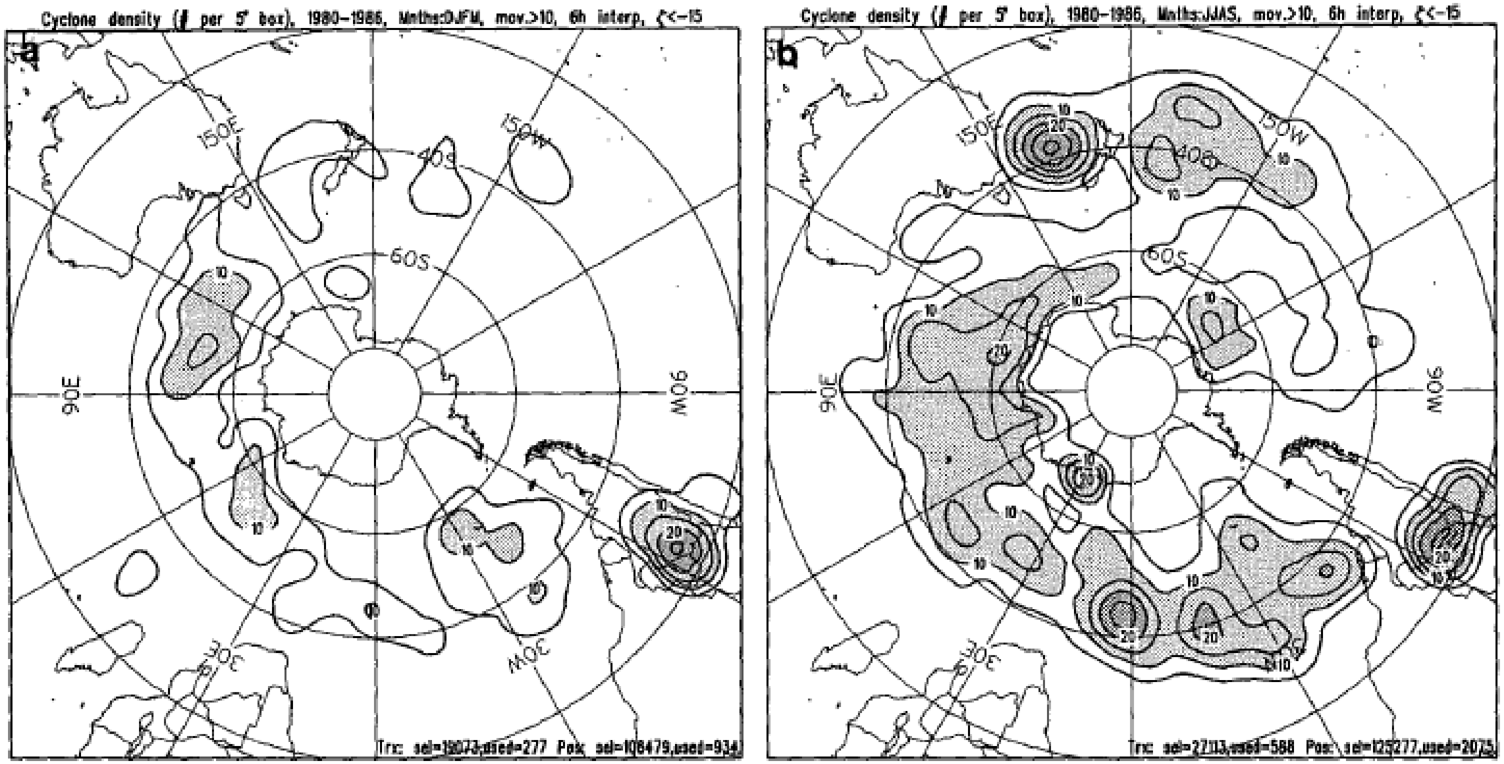


FIG. 13. Cyclone density for cyclones having central $\zeta_{w} < -15 \times 10^{-5}\ s^{-1}$ for (a) December, January, February, and March, and (b) June, July, August, and September for 1980–86 for cyclones moving a total distance greater than 10° of latitude. Six-hour interpolation is used. The contour interval is 5, with values greater than 10 (20) shaded (heavily).

# A New Perspective on Southern Hemisphere Storm Tracks

B. J. HOSKINS

*Department of Meteorology, University of Reading, Reading, United Kingdom*

K. I. HODGES

*Environmental Systems Science Centre, University of Reading, Reading, United Kingdom*

(Manuscript received 28 October 2004, in final form 11 May 2005)

Track upper level vortices

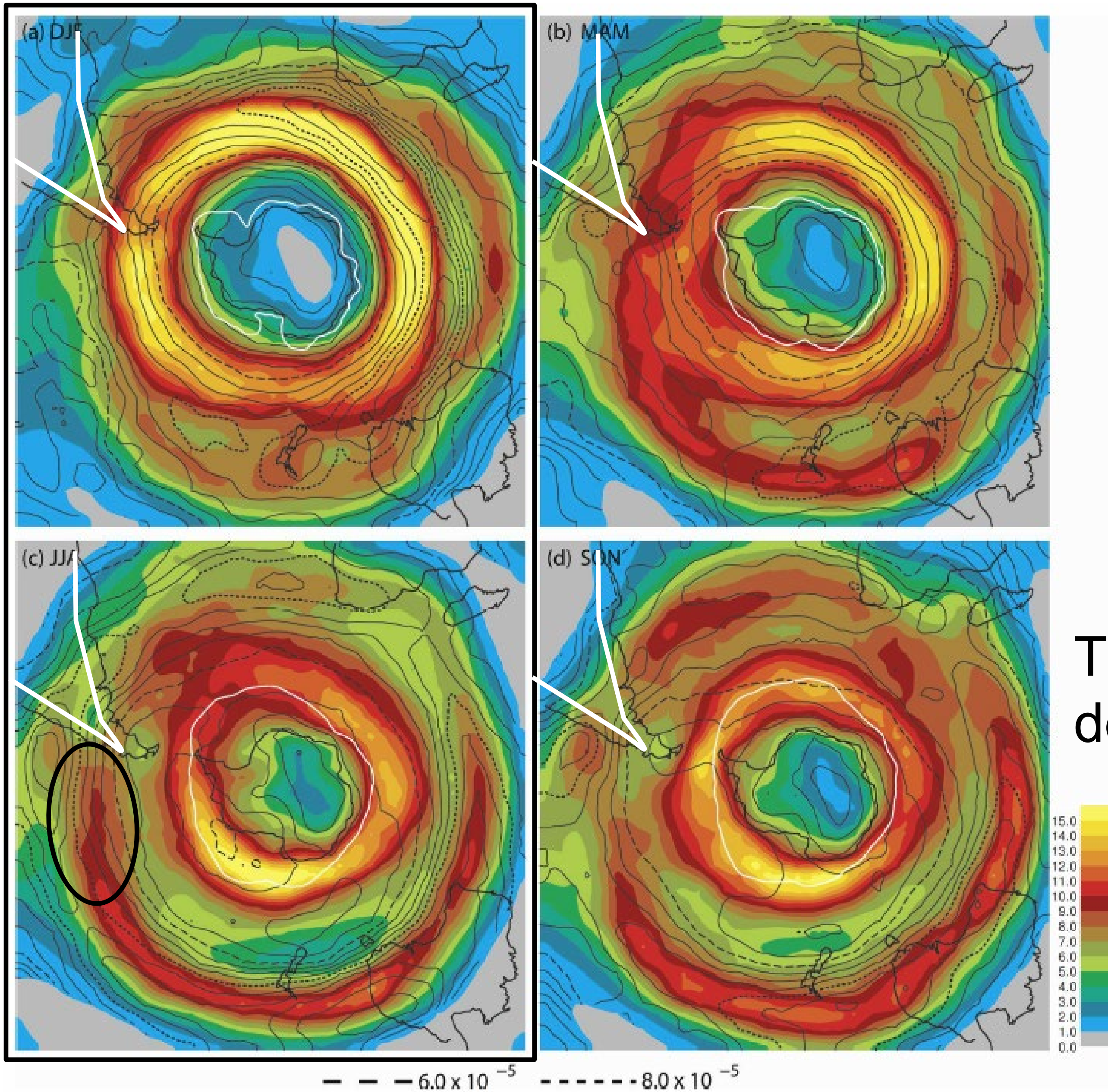


Track density

FIG. 10. Upper-tropospheric seasonal cycle of the SH storm track based on $\xi_{250}$: track density (color) and mean intensity (line contour) for (a) DJF (summer), (b) MAM (autumn), (c) JJA (winter), and (d) SON (spring). Track density is number density per month per unit area (unit area as in Fig. 4), and mean intensity is absolute relative to removed background with c.i. = $0.5 \times 10^{-5}$. The 50% sea ice boundary is delineated by the white line for each season.

Track lower level vortices

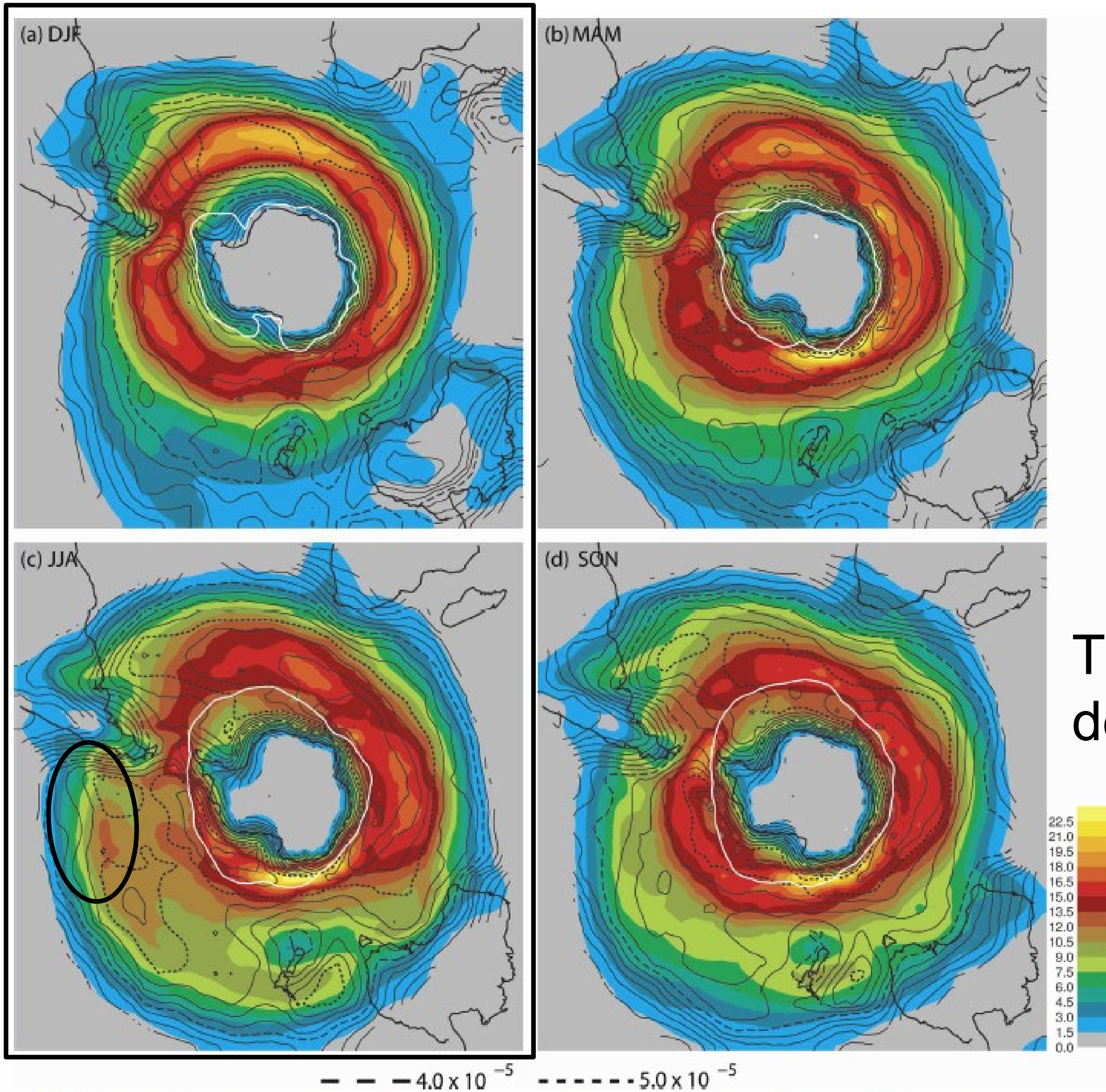


Track density

FIG. 11. Same as in Fig. 10, but for lower-tropospheric seasonal cycle based on $\xi_{850}$. Mean intensity is absolute relative to removed background with c.i. = $0.25 \times 10^{-5}$.

GEOPHYSICAL RESEARCH LETTERS, VOL. 38, L04809, doi:10.1029/2010GL046451, 2011

# A global climatology of atmospheric fronts

Gareth Berry,[1] Michael J. Reeder,[1] and Christian Jakob[1]

Received 9 December 2010; revised 13 January 2011; accepted 19 January 2011; published 25 February 2011.

GEOPHYSICAL RESEARCH LETTERS, VOL. 39, L10805, doi:10.1029/2012GL051736, 2012

# Relating global precipitation to atmospheric fronts

J. L. Catto,[1] C. Jakob,[2] G. Berry,[2] and N. Nicholls[1]

Received 19 March 2012; revised 11 April 2012; accepted 15 April 2012; published 18 May 2012.

[1] Atmospheric fronts are important for the day-to-day variability of weather in the midlatitudes, particularly during winter when extratropical storm-tracks are at their maximum intensity. Fronts are often associated with heavy rain, and strongly affect the local space-time distribution of rainfall. A recently developed objective front identification method that distinguishes between cold, warm and quasi-stationary fronts, is applied to reanalysis data and combined with a daily global gridded data set to investigate how precipitation around the globe is associated with atmospheric fronts. A large proportion (up to 90%) of rainfall in the major storm-track regions is associated with fronts, particularly cold and warm fronts. Precipitation over the oceanic storm-tracks is mostly associated with cold fronts, while over the Northern Hemisphere continents precipitation is mainly associated with warm fronts. There are seasonal and regional variations in the proportion of precipitation associated with fronts.

**Citation:** Catto, J. L., C. Jakob, G. Berry, and N. Nicholls (2012), Relating global precipitation to atmospheric fronts, *Geophys. Res. Lett.*, *39*, L10805, doi:10.1029/2012GL051736.

were also found to be where the frontal intensity is greatest [*Simmonds et al.*, 2011].

[4] Although the regions of maximum annual average precipitation occur in the tropics [*Garreaud*, 2007], there are also large regions of high values of annual average precipitation over the midlatitude storm track regions. Much of the rainfall in the midlatitudes has long been known to be associated with the passage of frontal systems, as shown in *Bjerknes and Solberg* [1922]. The distribution of precipitation around frontal systems has since been investigated using case studies [e.g., *Browning and Roberts*, 1994] and compositing techniques [e.g., *Field and Wood*, 2007]. On regional scales studies have been performed to attribute precipitation to fronts or other synoptic activity [e.g., *Pook et al.*, 2006]. Studies of particular cases or regions are often subjective in nature and as such are not able to be reproduced or extended to global analysis. For this reason the volume of global precipitation associated with fronts has yet to be quantified.

[5] Given the importance of fronts to local weather in many regions, it is feasible that some of the observed trends

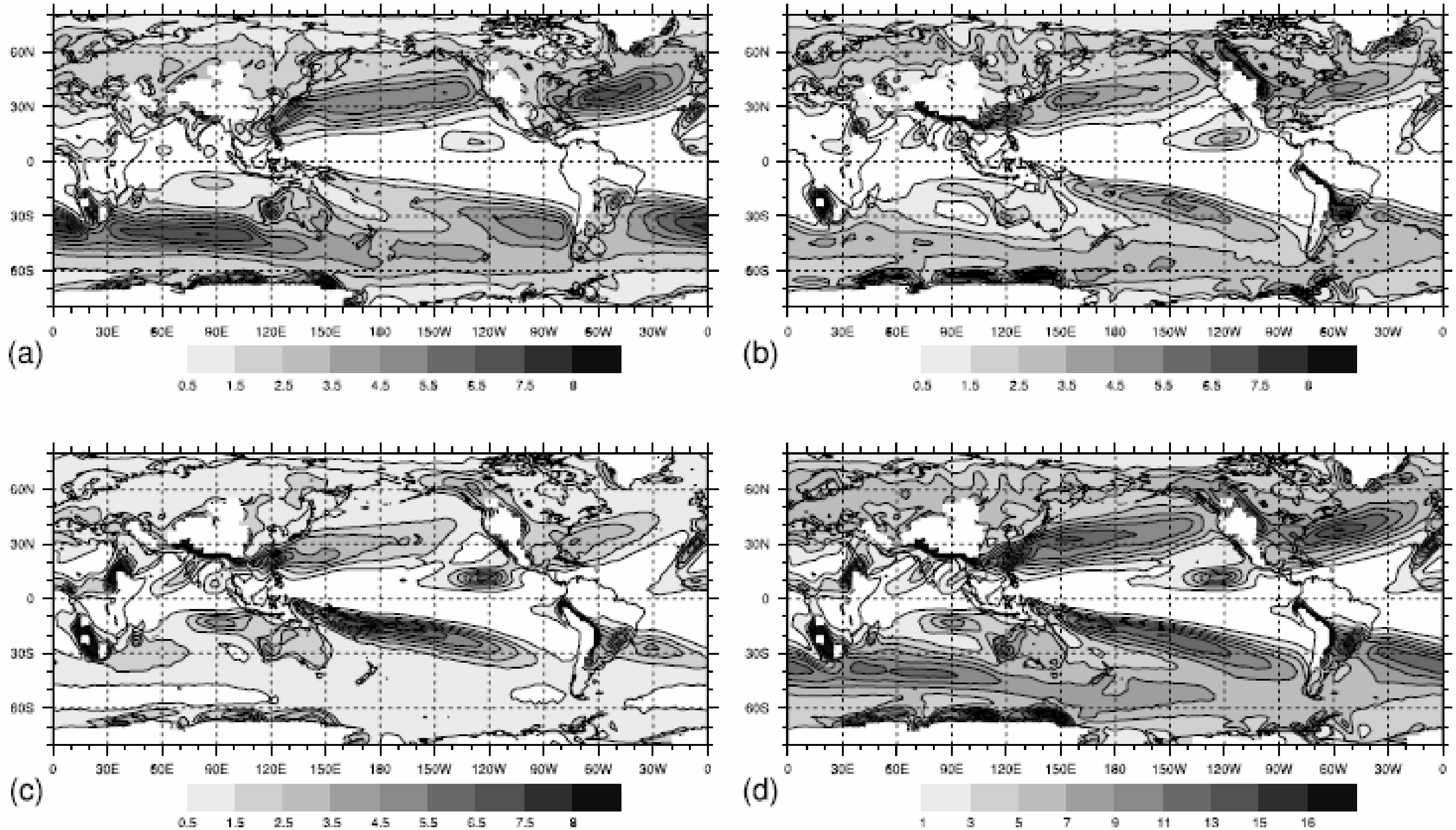


**Figure 2.** Annual mean front frequency of (a) cold (b) warm (c) quasi-stationary and (d) the sum of all fronts in the ERA-40 reanalysis. Units are percentage time at which an objectively identified front was located within each grid box. Scales are displayed under each panel.

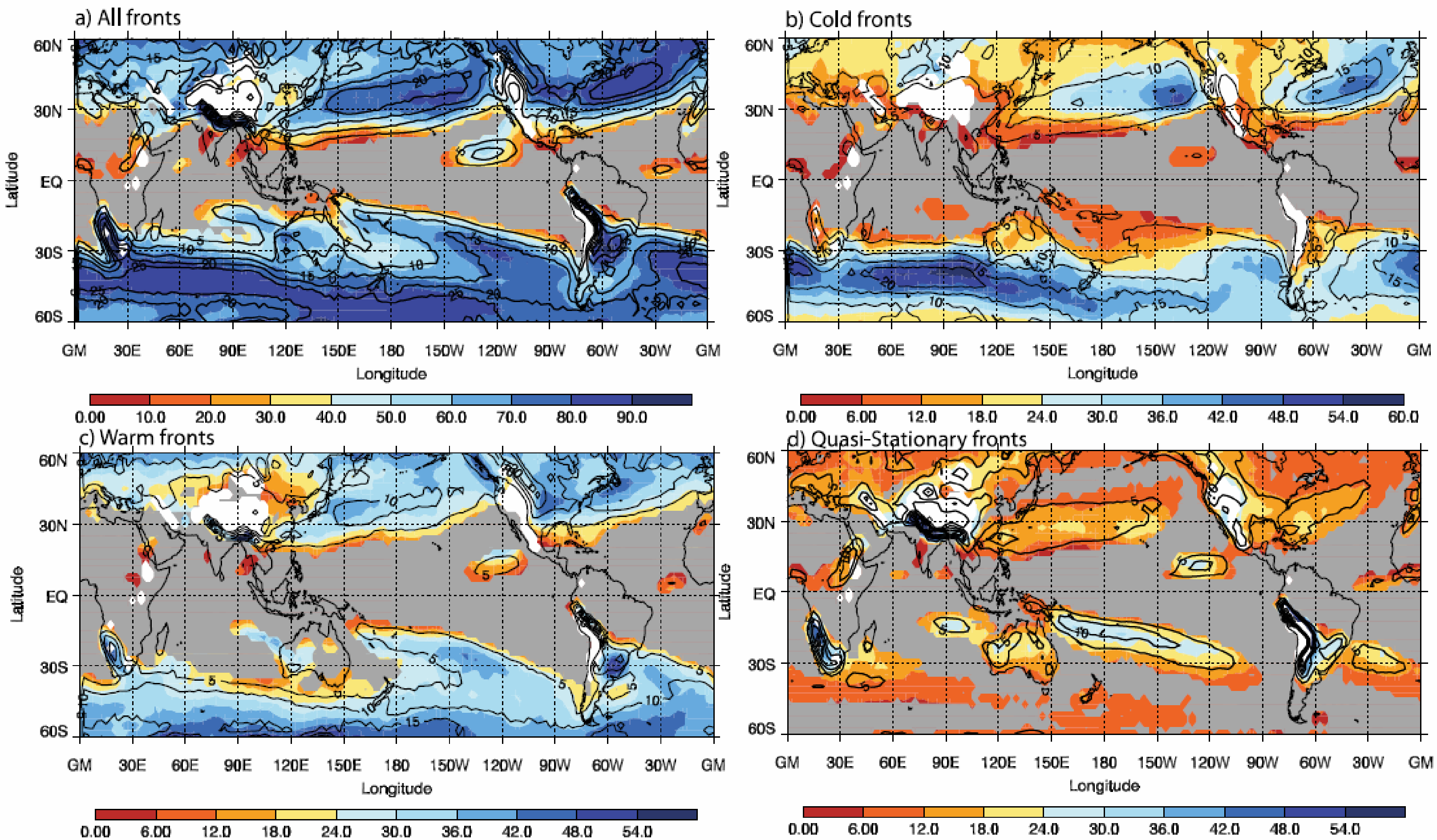


**Figure 1.** Colors show annual proportion of precipitation that occurs with (a) any front, (b) cold front, (c) warm front, (d) quasi-stationary front within a 5° box. The black contours show the front frequency as a percentage time that a front was located within each grid box. Polewards of ±60° has been cut off due to problems with the convergence of the meridians. Regions where the surface topography is higher than 1.5 km (850 hPa in a standard atmosphere) have been blanked out, and areas where the front frequency is less than 3% have been shaded grey.

# Tormentas de invierno Chile centro-sur

*René D. Garreaud*
Departamento de Geofísica
Universidad de Chile

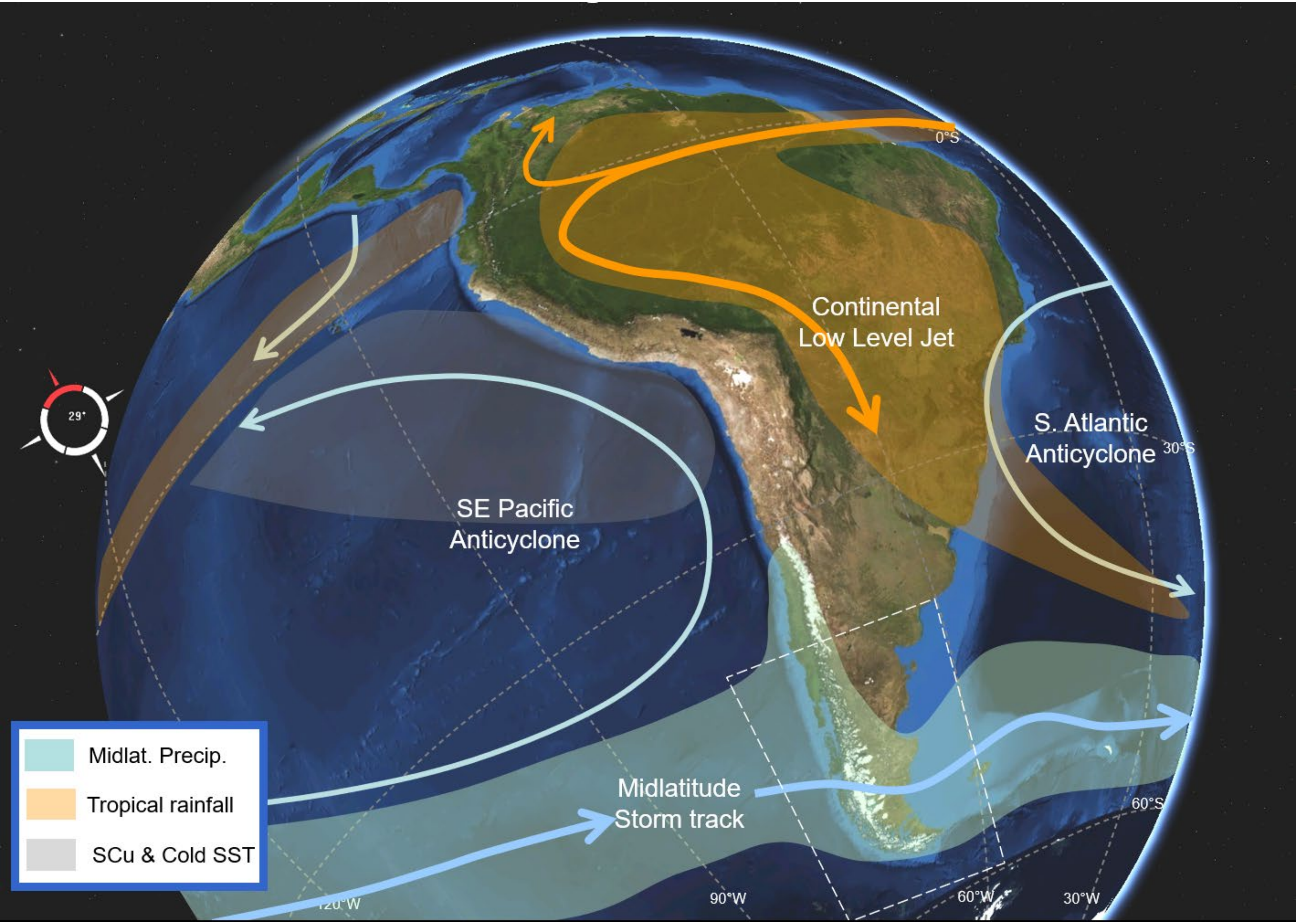

0°S
Continental
Low Level Jet
S. Atlantic
Anticyclone
30°S
SE Pacific
Anticyclone
29°
Midlat. Precip.
Tropical rainfall
SCu & Cold SST
Midlatitude
Storm track
60°S
120°W
90°W
60°W
30°W

# Precipitacion en Latitudes medias

Modest annual cycle in the extratropics

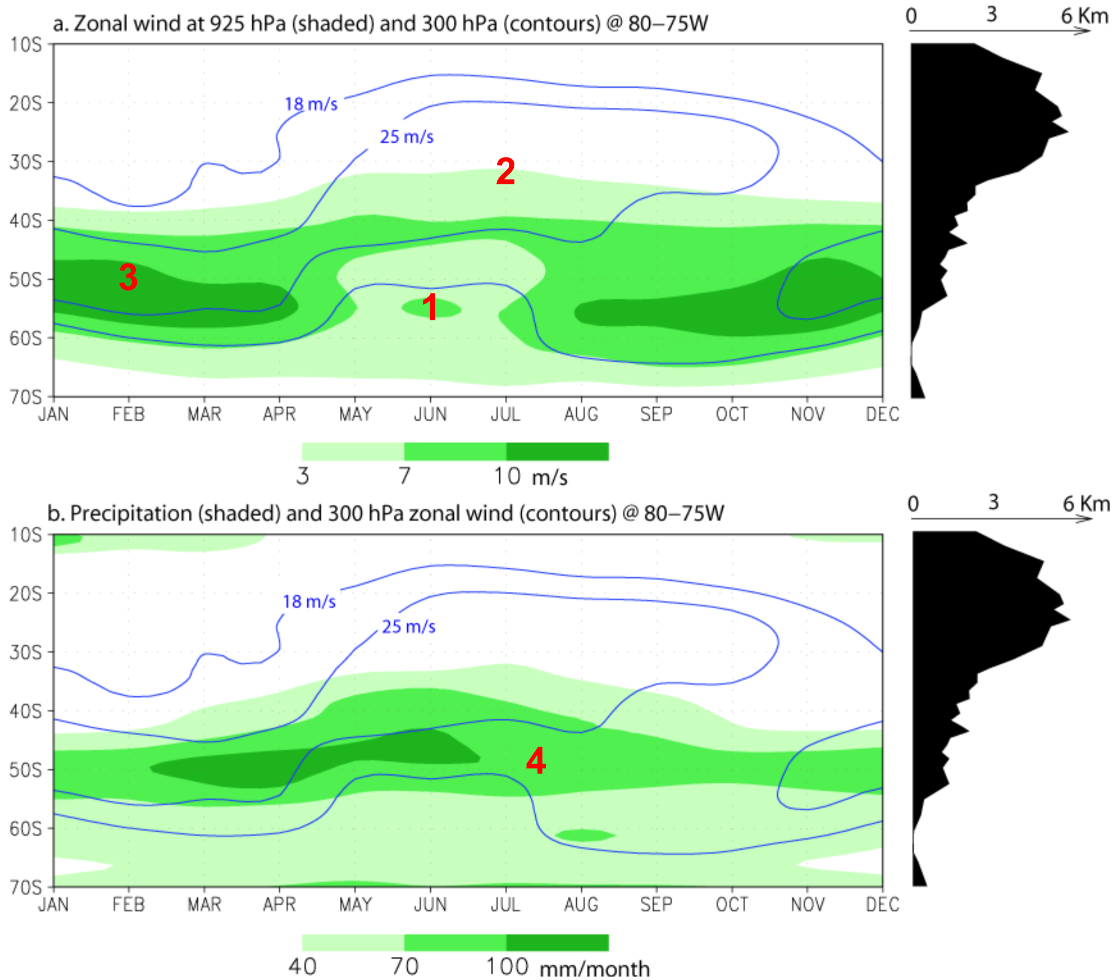

# Condiciones de gran escala

# Características de Escala Sinóptica

Análisis de agrupamiento objetivo (cluster análisis) basado en los campos de presión de superficie y geopotencial a 500 hPa revelan 5 situaciones sinópticas diferentes que se asocian con precipitación en Chile central.

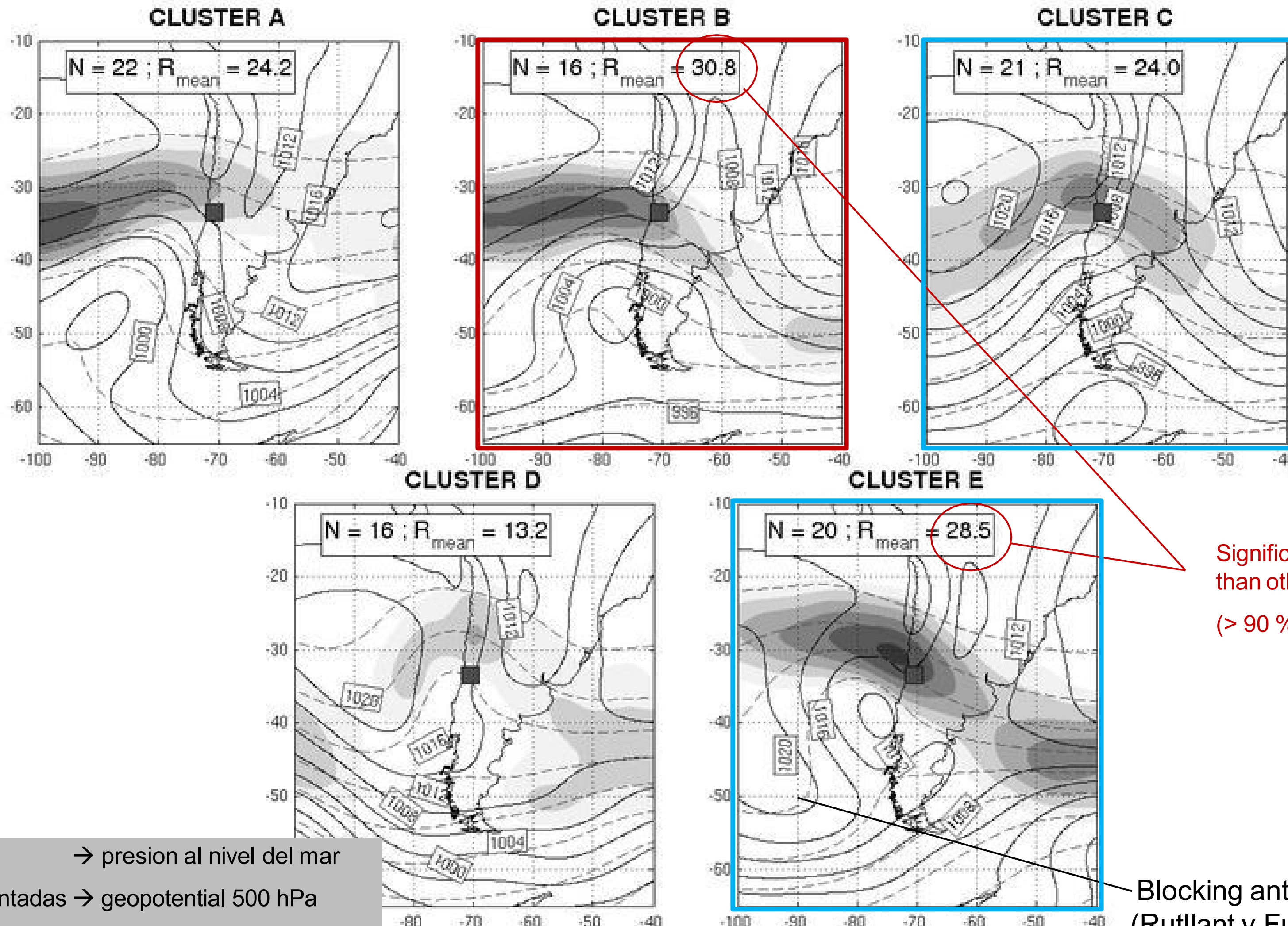


Significantly higher than other clusters

(> 90 % significance)

Blocking anticyclone?
(Rutllant y Fuenzalida, 1991

Líneas sólidas → presion al nivel del mar

Líneas segmentadas → geopotential 500 hPa

Achurados grises → Viento 300 hPa > 35 m/s

Figure 5’: COL
(7 Mar 2008)

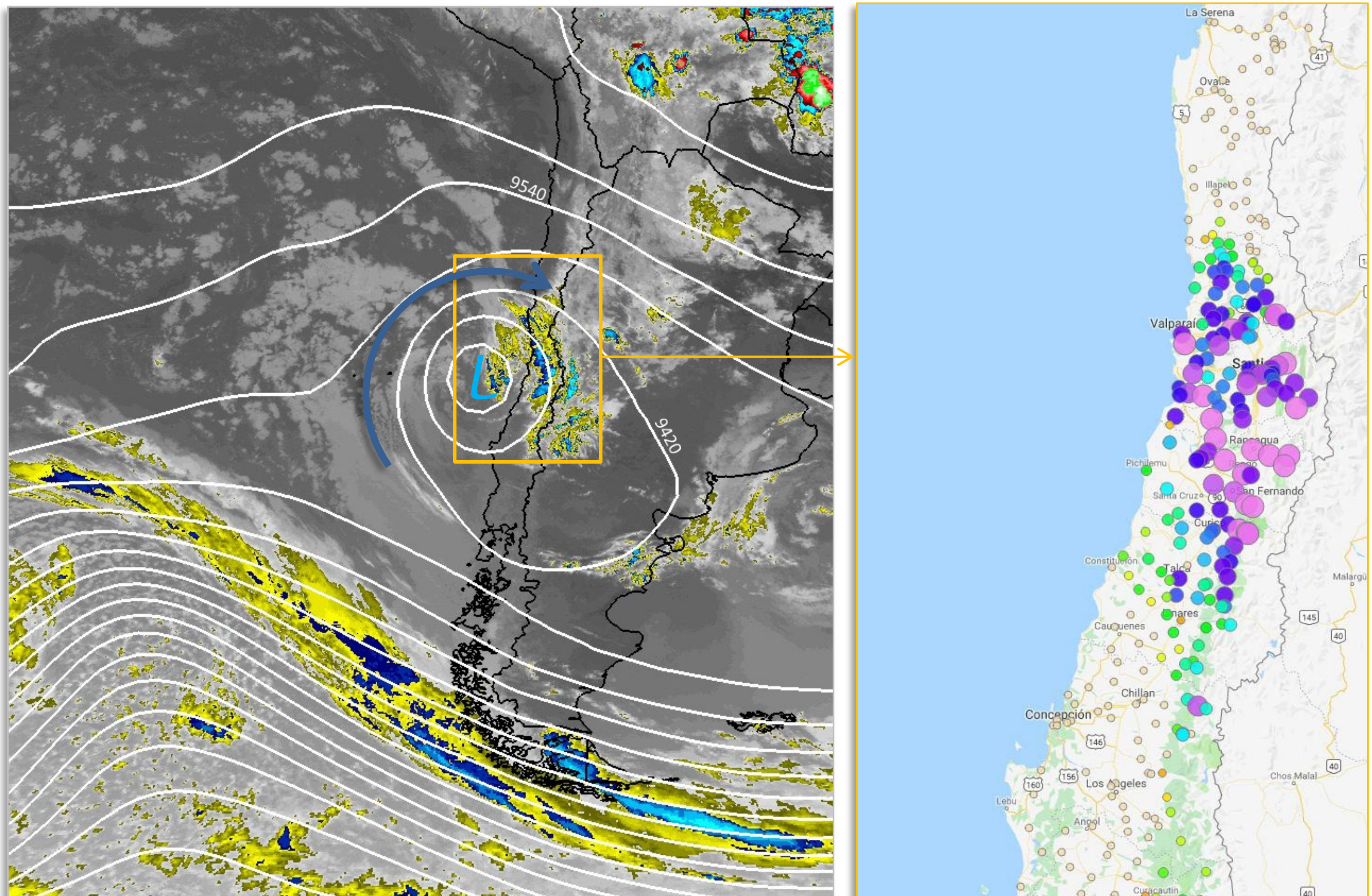

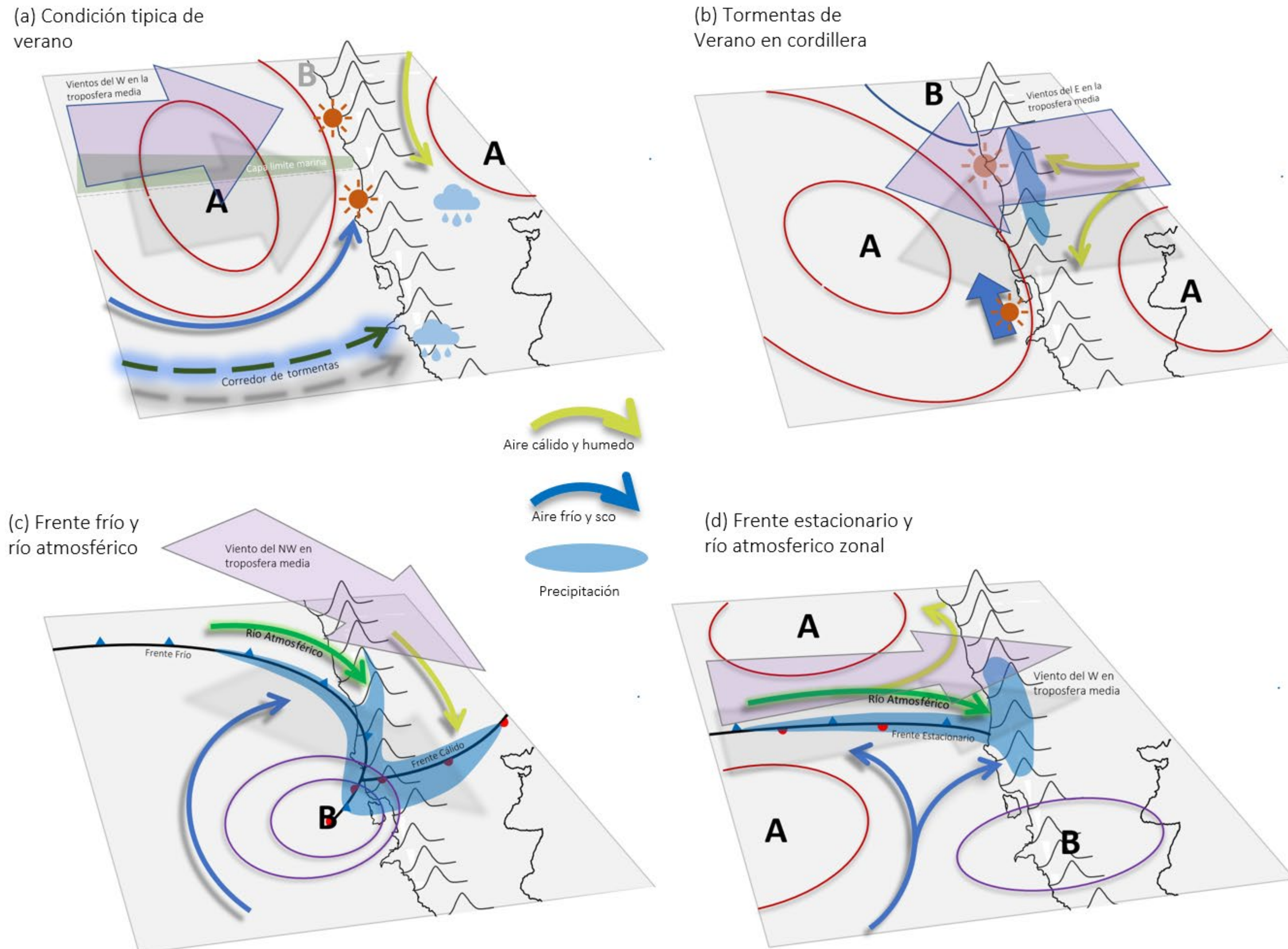

(a) Condición tipica de verano
Vientos del W en la troposfera media
B
A
Capa limite marina
A
Corredor de tormentas
(b) Tormentas de Verano en cordillera
B
Vientos del E en la troposfera media
A
A
Aire cálido y humedo
Aire frío y sco
Precipitación
(c) Frente frío y río atmosférico
Viento del NW en troposfera media
Frente Frío
Río Atmosférico
Frente Cálido
B
(d) Frente estacionario y río atmosferico zonal
A
Viento del W en troposfera media
Río Atmosférico
Frente Estacionario
A
B

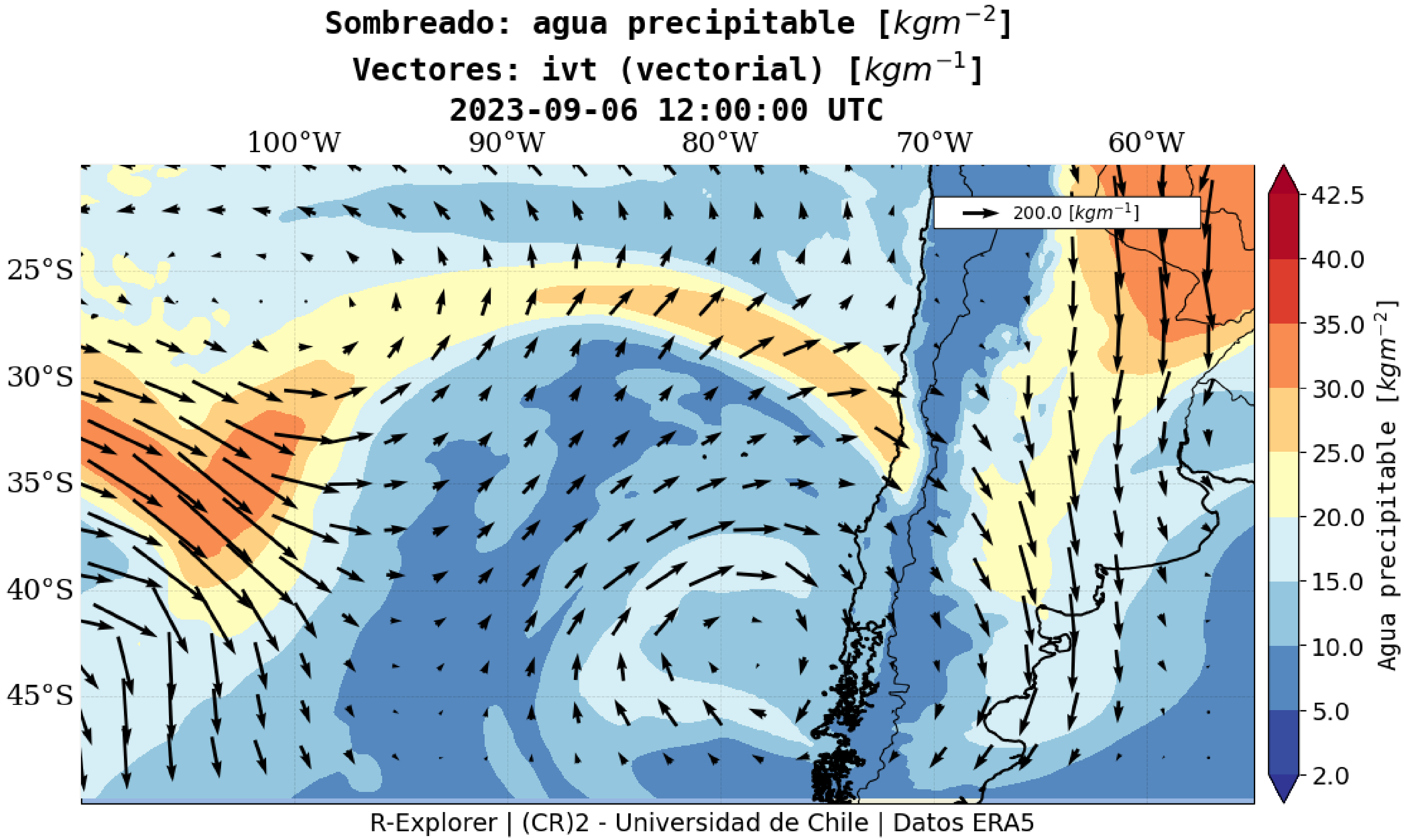
Sombreado: agua precipitable [$kgm^{-2}$]
Vectores: ivt (vectorial) [$kgm^{-1}$]
2023-09-06 12:00:00 UTC
100°W
90°W
80°W
70°W
60°W
25°S
30°S
35°S
40°S
45°S
200.0 [$kgm^{-1}$]
42.5
40.0
35.0
30.0
25.0
20.0
15.0
10.0
5.0
2.0
Agua precipitable [$kgm^{-2}$]
R-Explorer | (CR)2 - Universidad de Chile | Datos ERA5

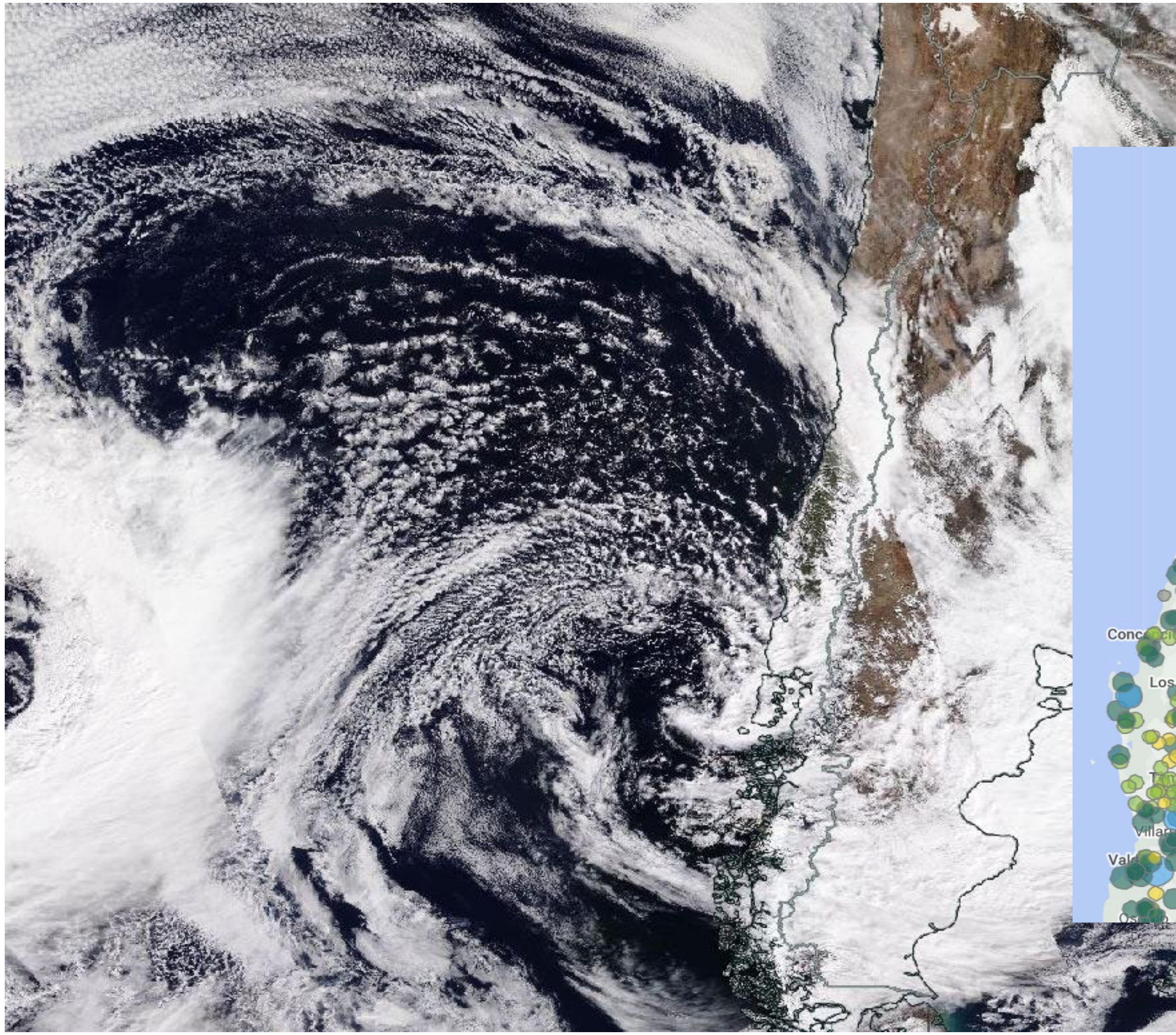

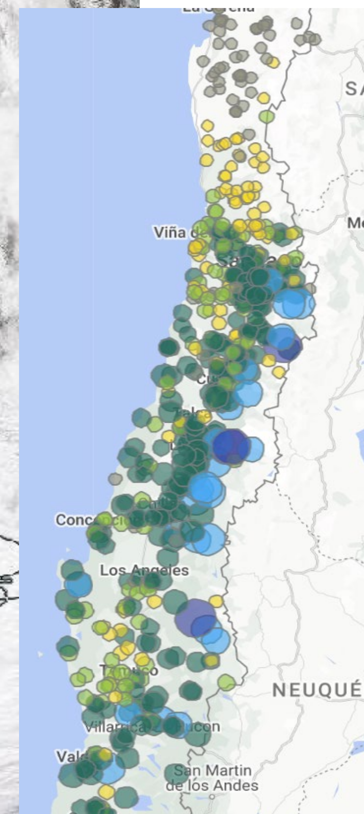
Los Angeles
NEUQUÉN
San Martin
de los Andes

# Río atmosférico inclinado delante de un frente frío

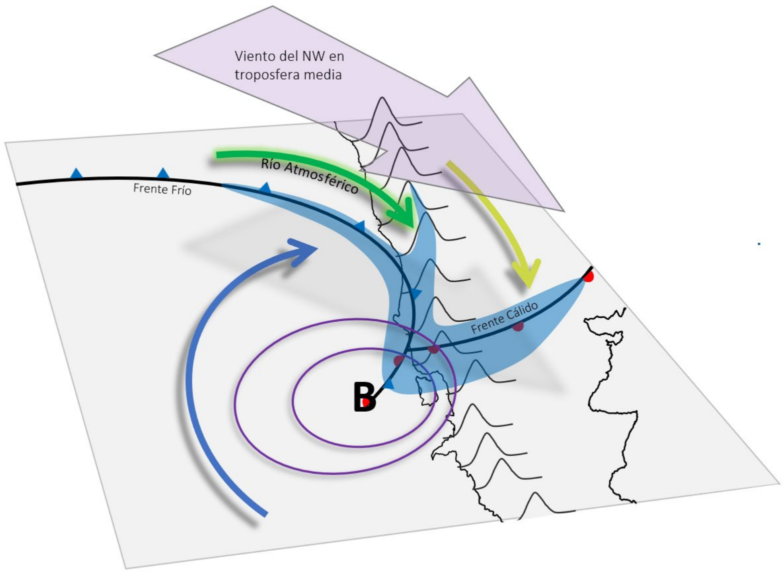


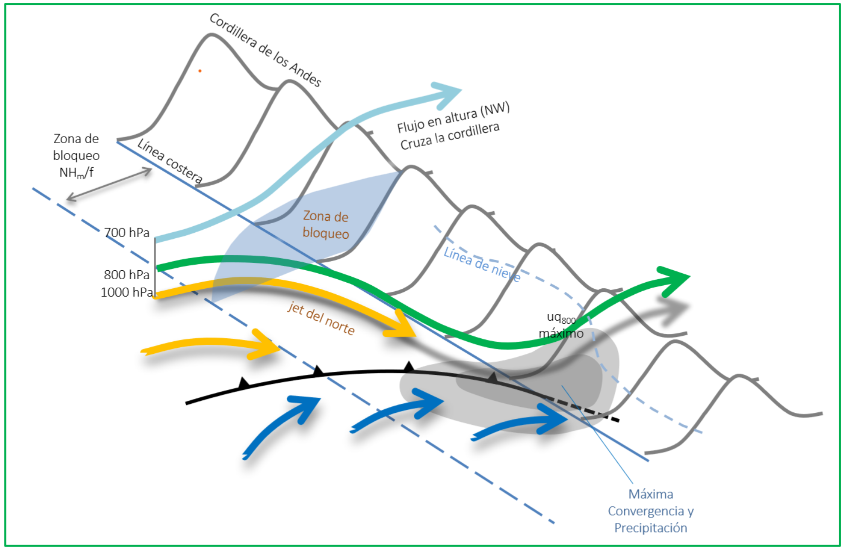

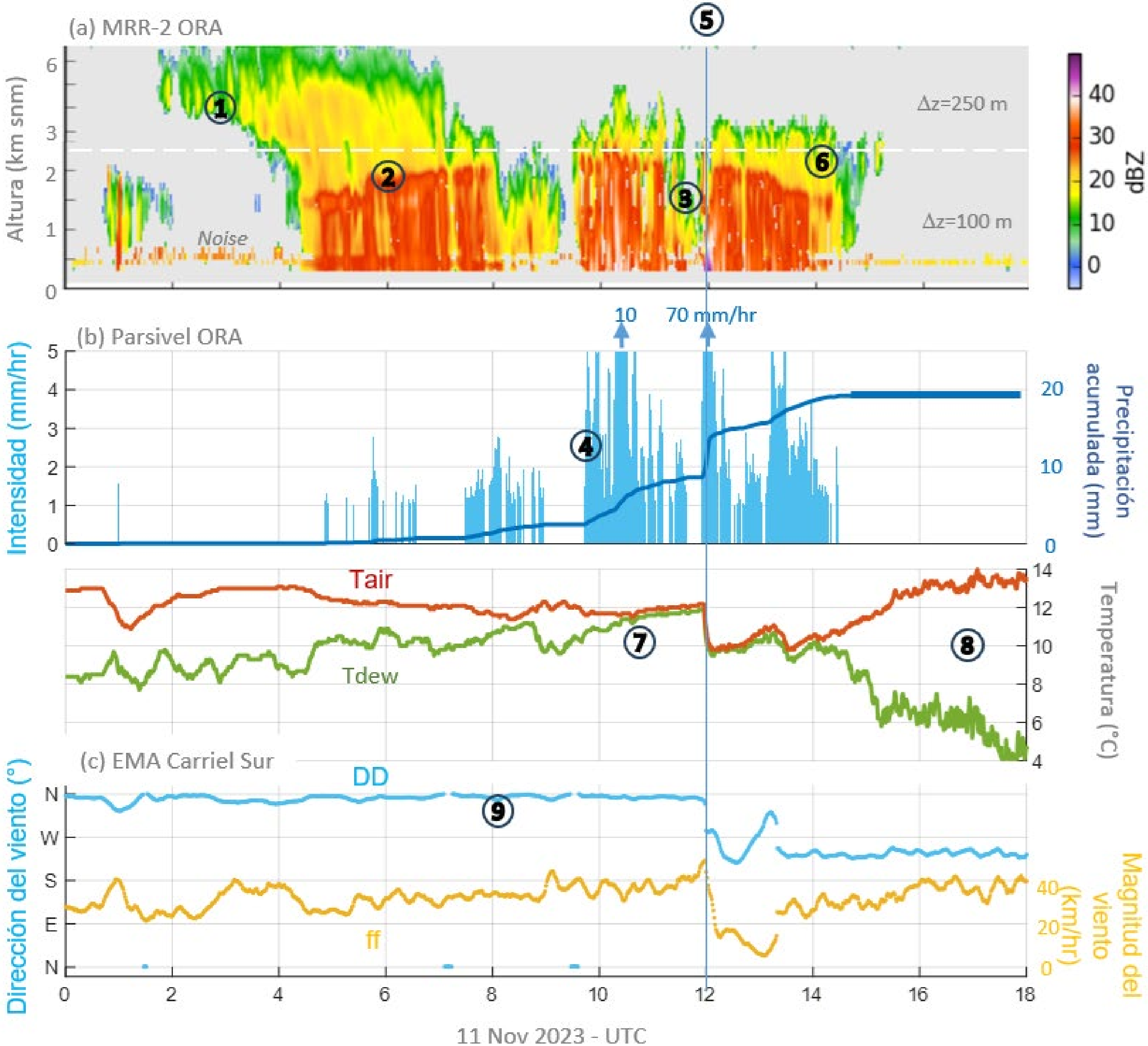

(a) MRR-2 ORA
Altura (km snm)
Δz=250 m
Δz=100 m
Noise
dBZ
(b) Parsivel ORA
10
70 mm/hr
Intensidad (mm/hr)
Precipitación acumulada (mm)
Tair
Tdew
Temperatura (°C)
(c) EMA Carriel Sur
DD
ff
Dirección del viento (°)
Magnitud del viento (km/hr)
11 Nov 2023 - UTC

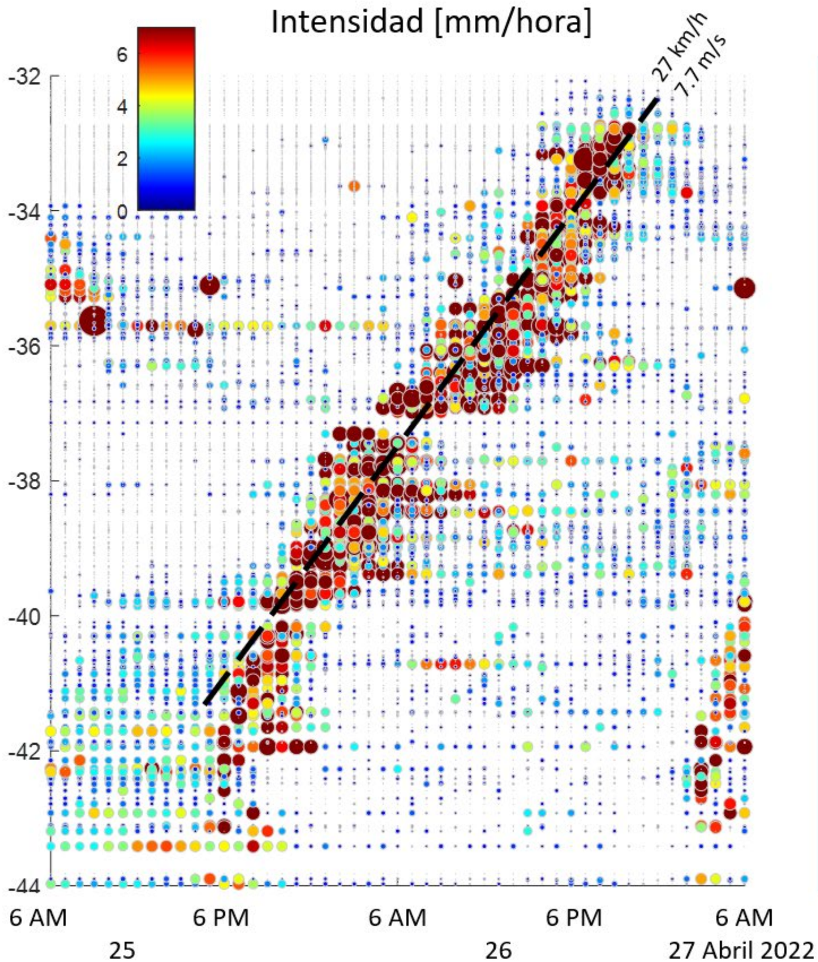
Intensidad [mm/hora]
6
4
2
0
27 km/h
7.7 m/s
-32
-34
-36
-38
-40
-42
-44
6 AM
6 PM
6 AM
6 PM
6 AM
25
26
27 Abril 2022

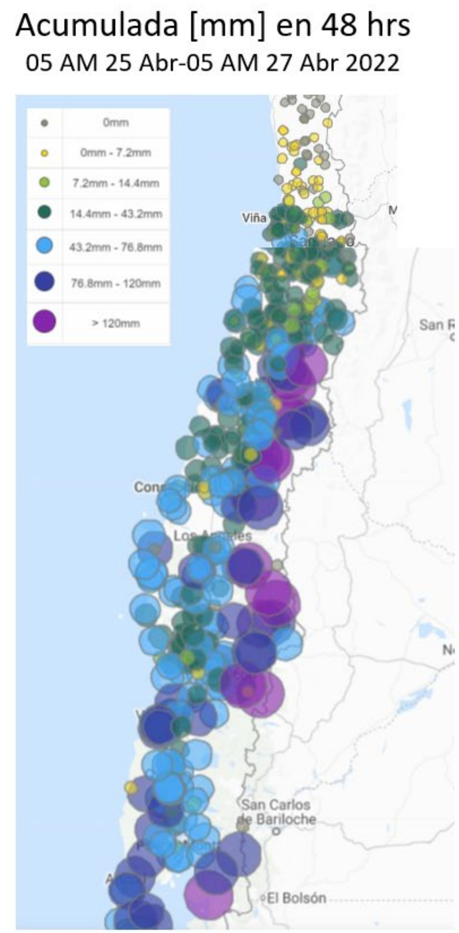
Acumulada [mm] en 48 hrs
05 AM 25 Abr-05 AM 27 Abr 2022
0mm
0mm - 7.2mm
7.2mm - 14.4mm
14.4mm - 43.2mm
43.2mm - 76.8mm
76.8mm - 120mm
> 120mm
Viña
San Carlos de Bariloche
El Bolsón

# Condiciones locales (superficie + altura) durante tormentas en centro-sur de Chile

# Condiciones Locales
## Perfiles en Santo Domingo cuando llueve en Santiago…



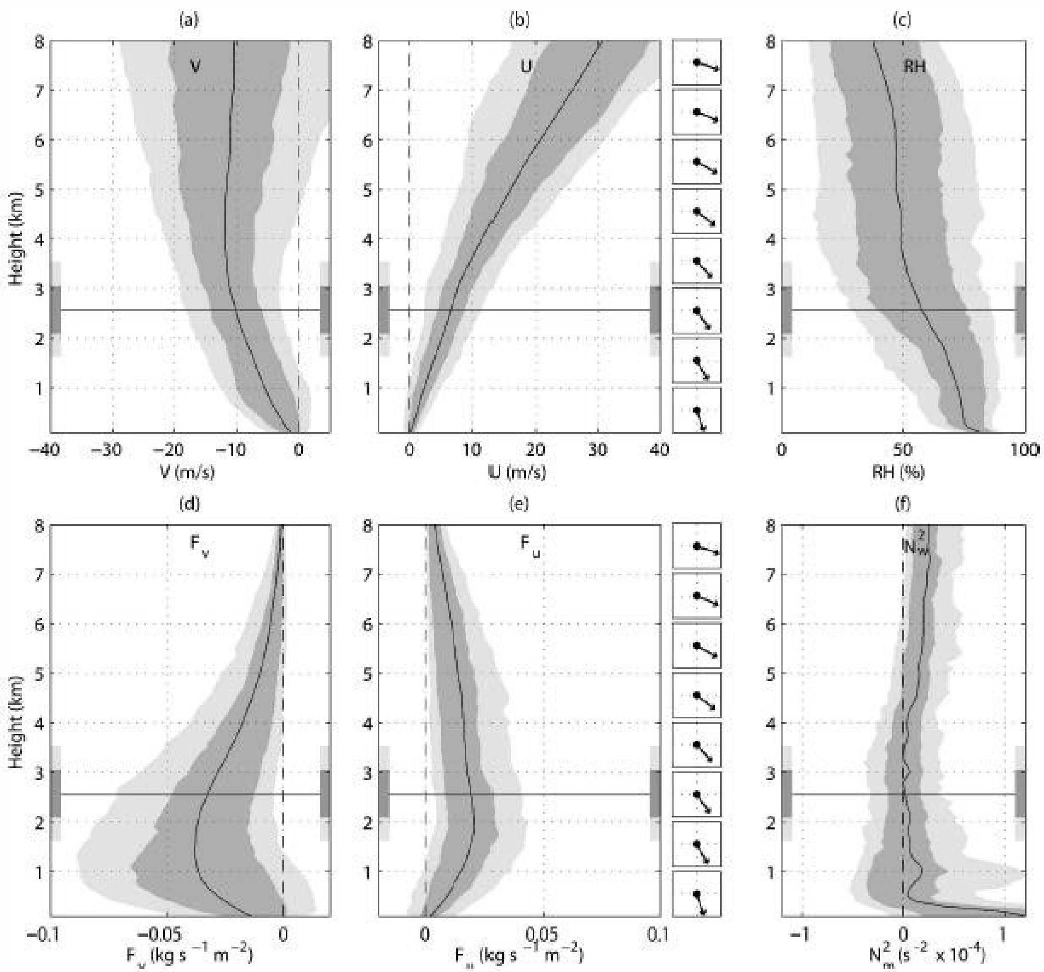


FIG. 6. (a)–(d) Vertical profiles of coastal radiosonde measurements of selected atmospheric variables during rainfall episodes. The solid line indicates the mean value, the dark gray region indicates the interquartile range, and the light gray region indicates the 5%–95% percentile range. The gray horizontal line is the mean height of the freezing level, and the dark and light gray bars on either side of the plot show its interquartile and 5%–95% percentile ranges, respectively. The arrows left of (a) and (d) indicate the direction of the wind and flux vectors. The variables are defined in Table 3.

# Condiciones Locales (Sonda de SDO, precipitación en Santiago)

Progresión temporal de las anomalías* de algunas variables medidas por radiosonda, de 3 días antes hasta tres días después  del evento de lluvia.

Dia 0 (PP en Stgo)

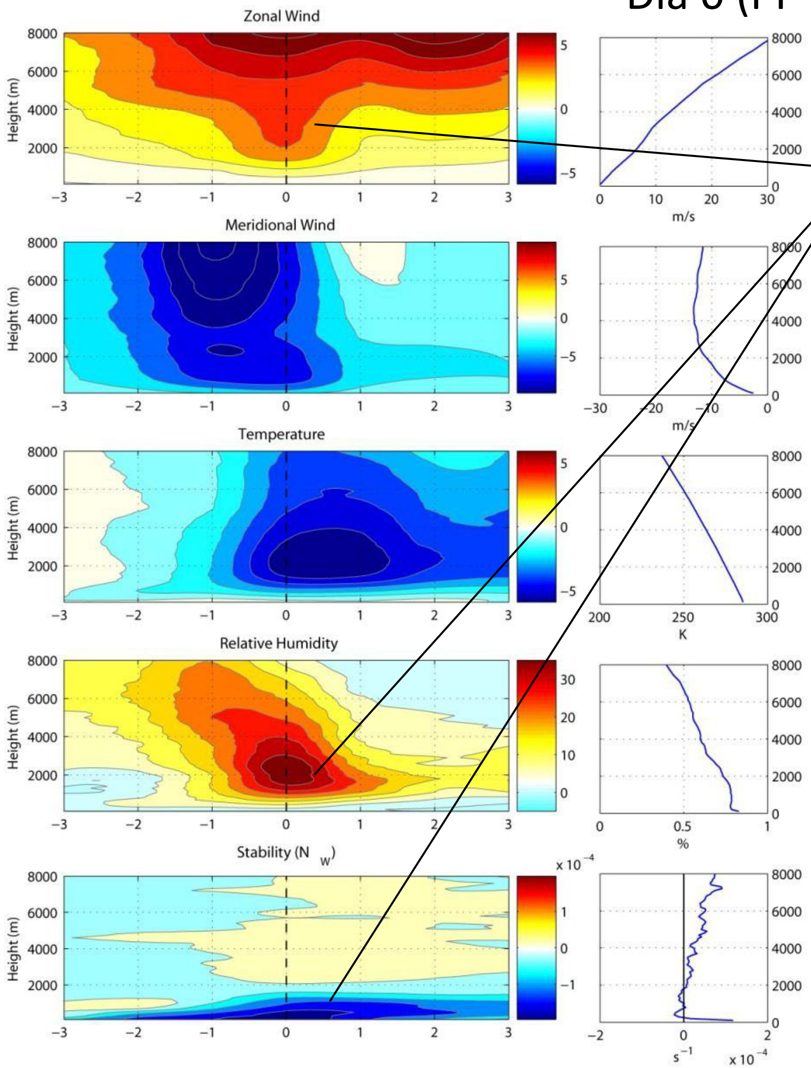


Factores mas importantes para la generación de lluvia orográfica

- Viento promedio hacia la Cordillera
- Aire húmedo
- Inestabilidad condicional

*Anomalías con respecto al perfil promedio de invierno (Abril - Septiembre)

Zonal wind (shaded), T=0° (White), q=5 g/Kg (blue), U=5 m/s (black) – Full Topo

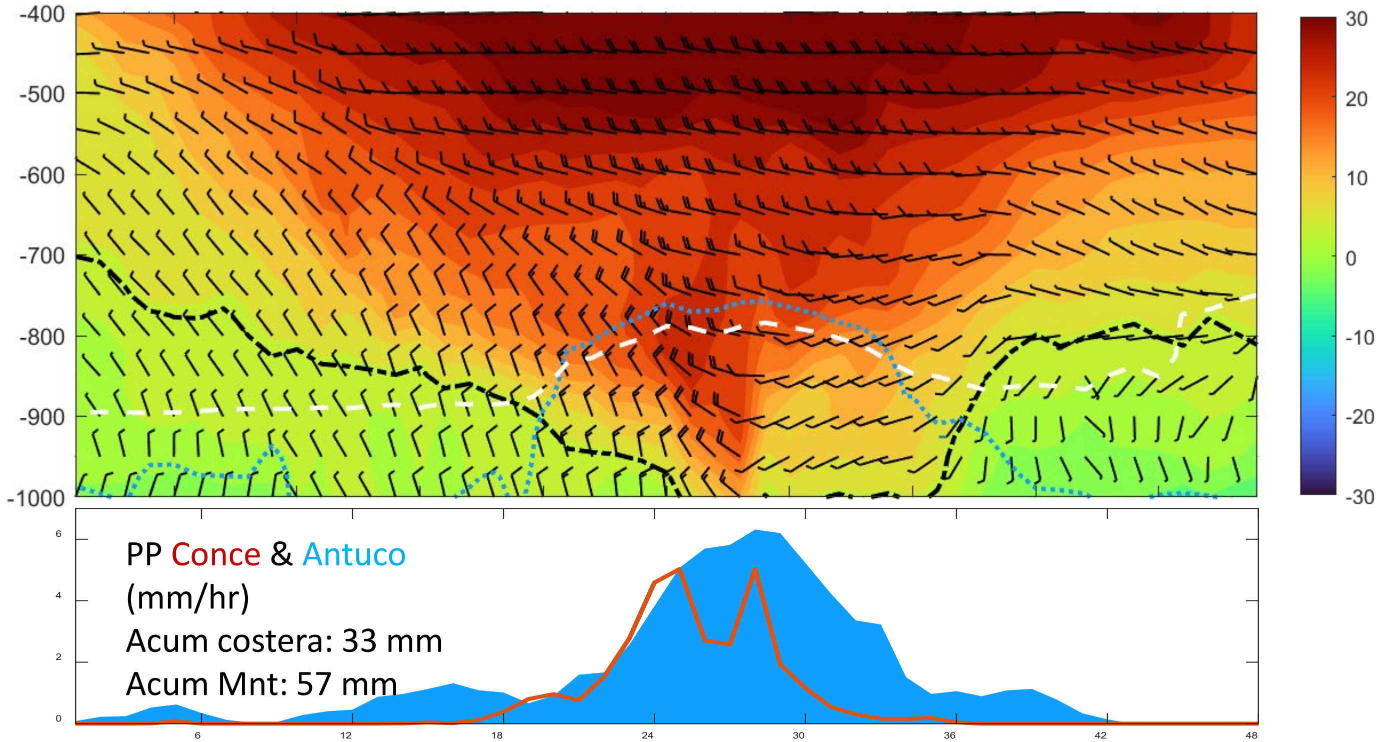

Fulltopo

Zonal wind (shaded), T=0° (White), q=5 g/Kg (blue), U=5 m/s (black)

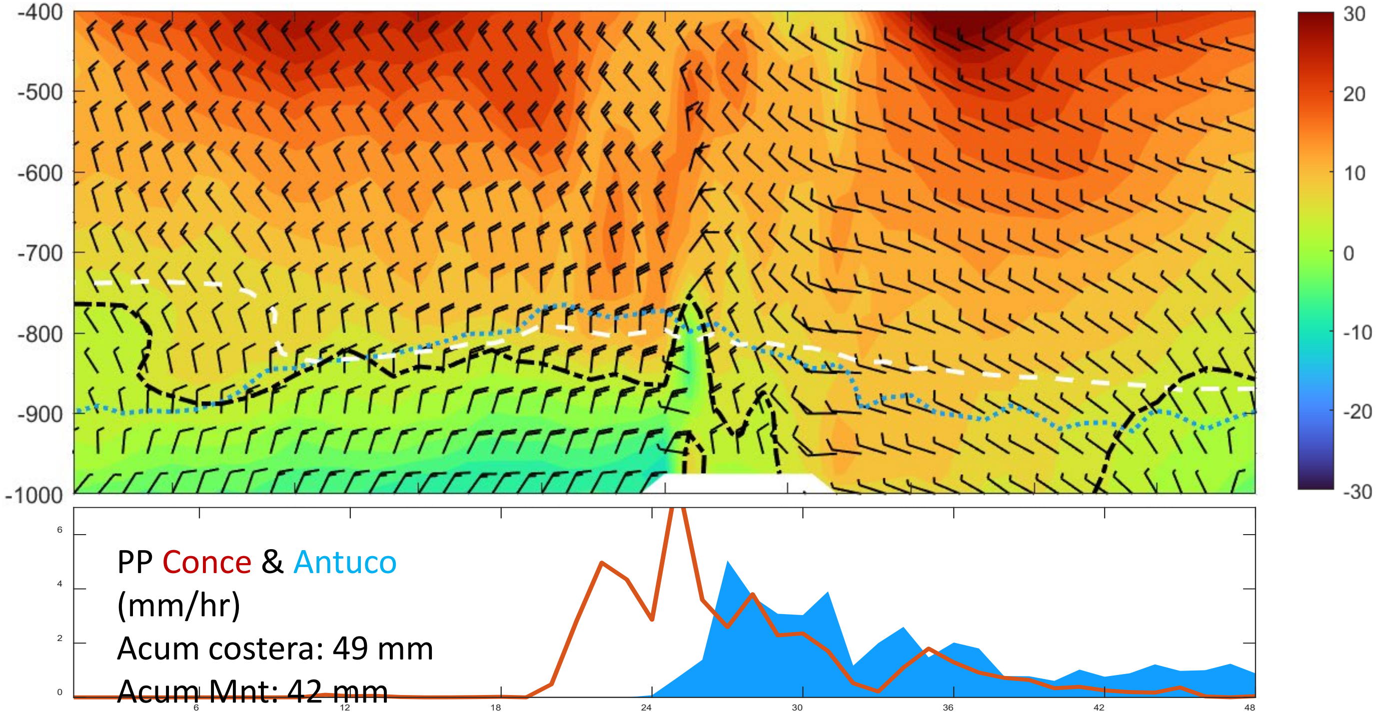

# Warm and cold winter rainstorms

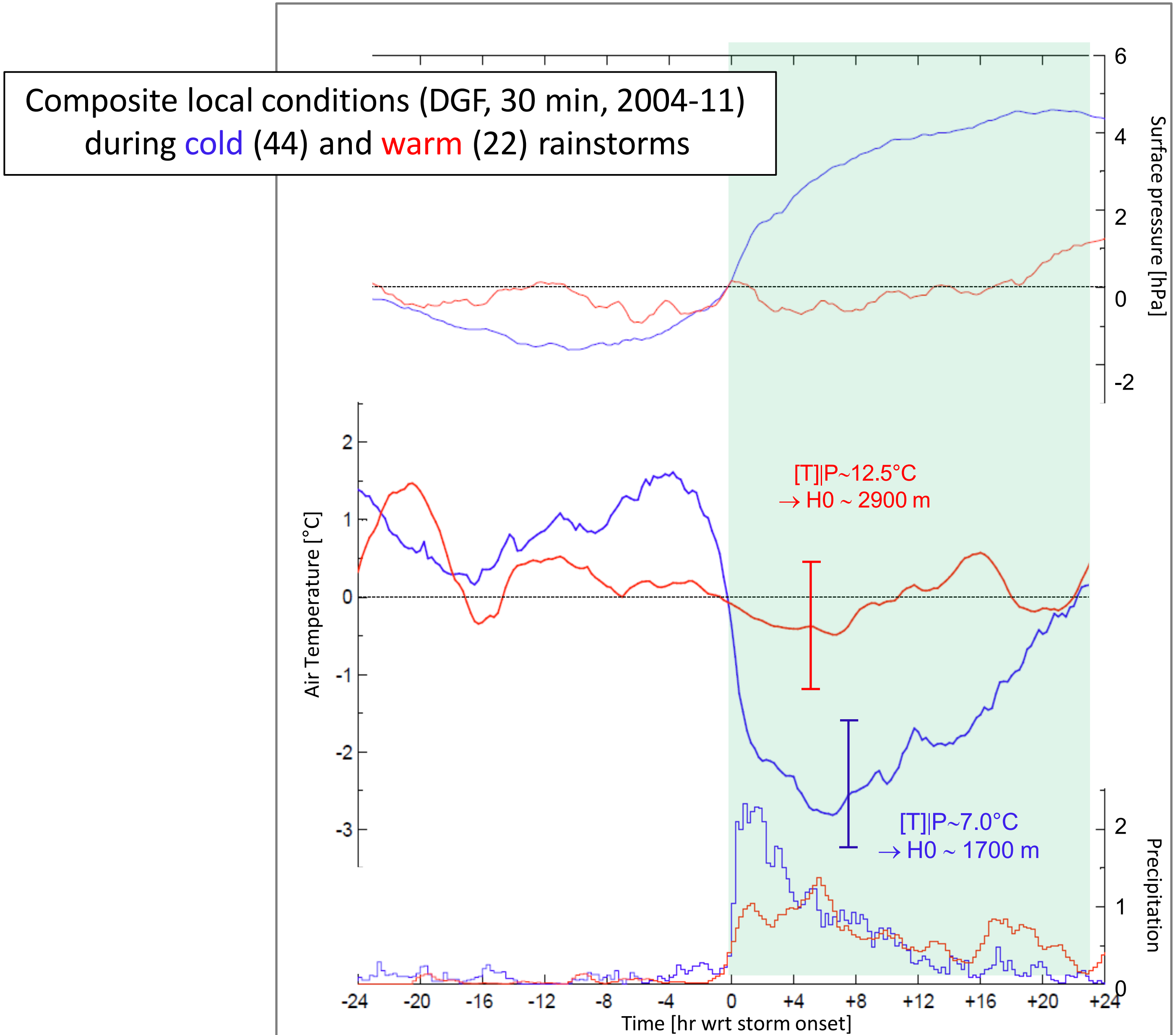

# Condiciones Locales (Nahuelbuta, al sur del BioBio)

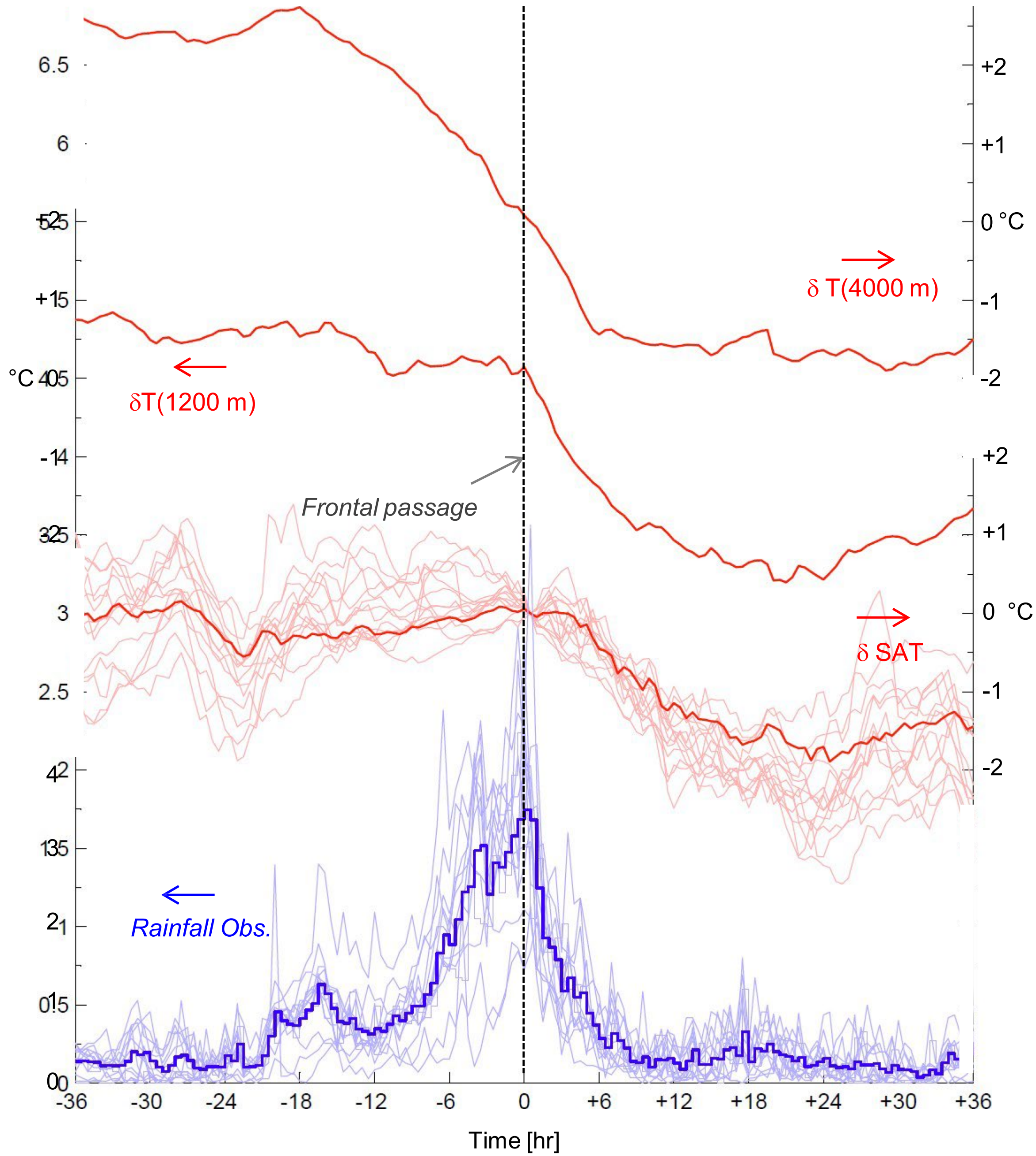

# Condiciones Locales (Nahuelbuta, al sur del BioBio)

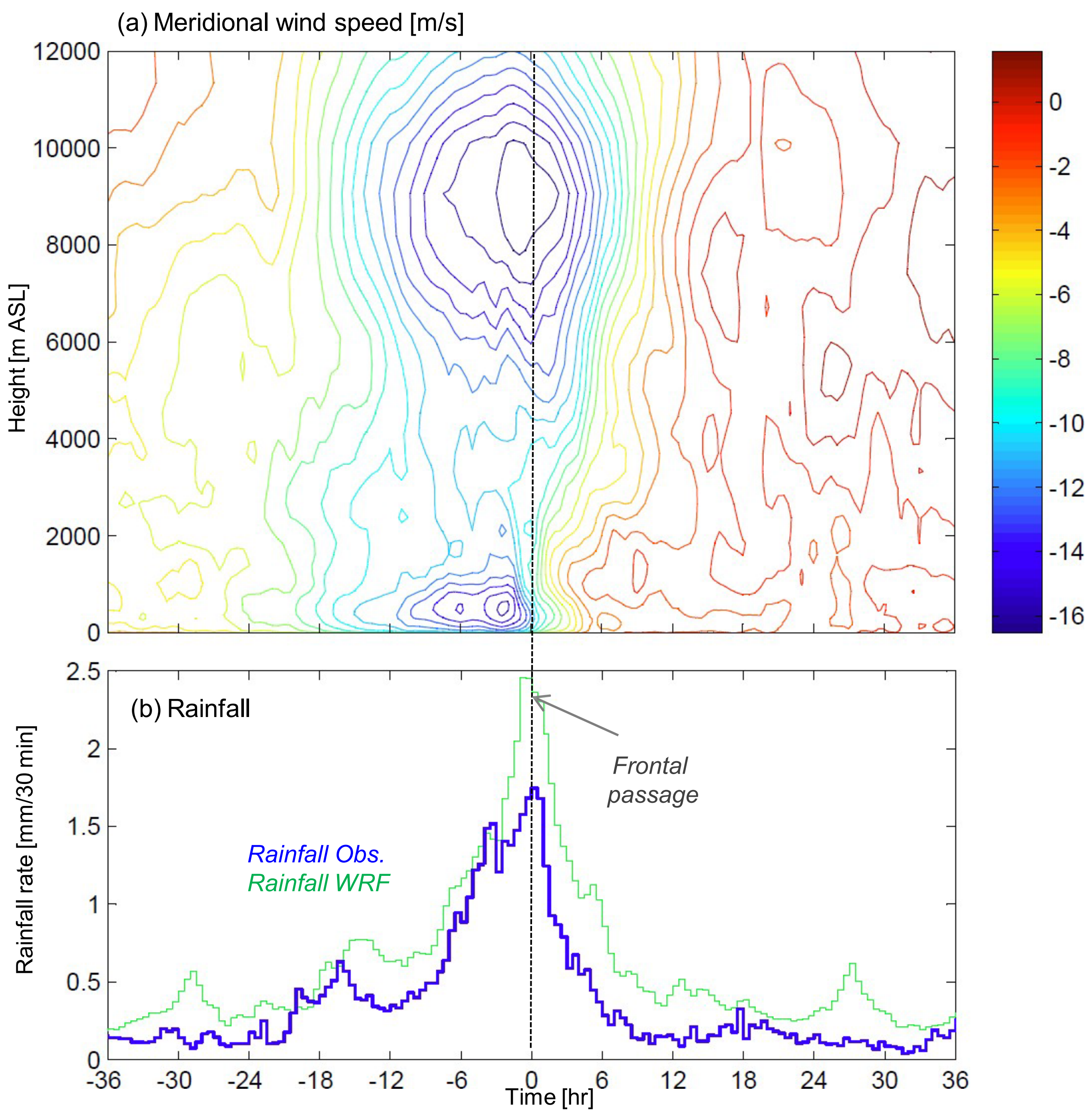

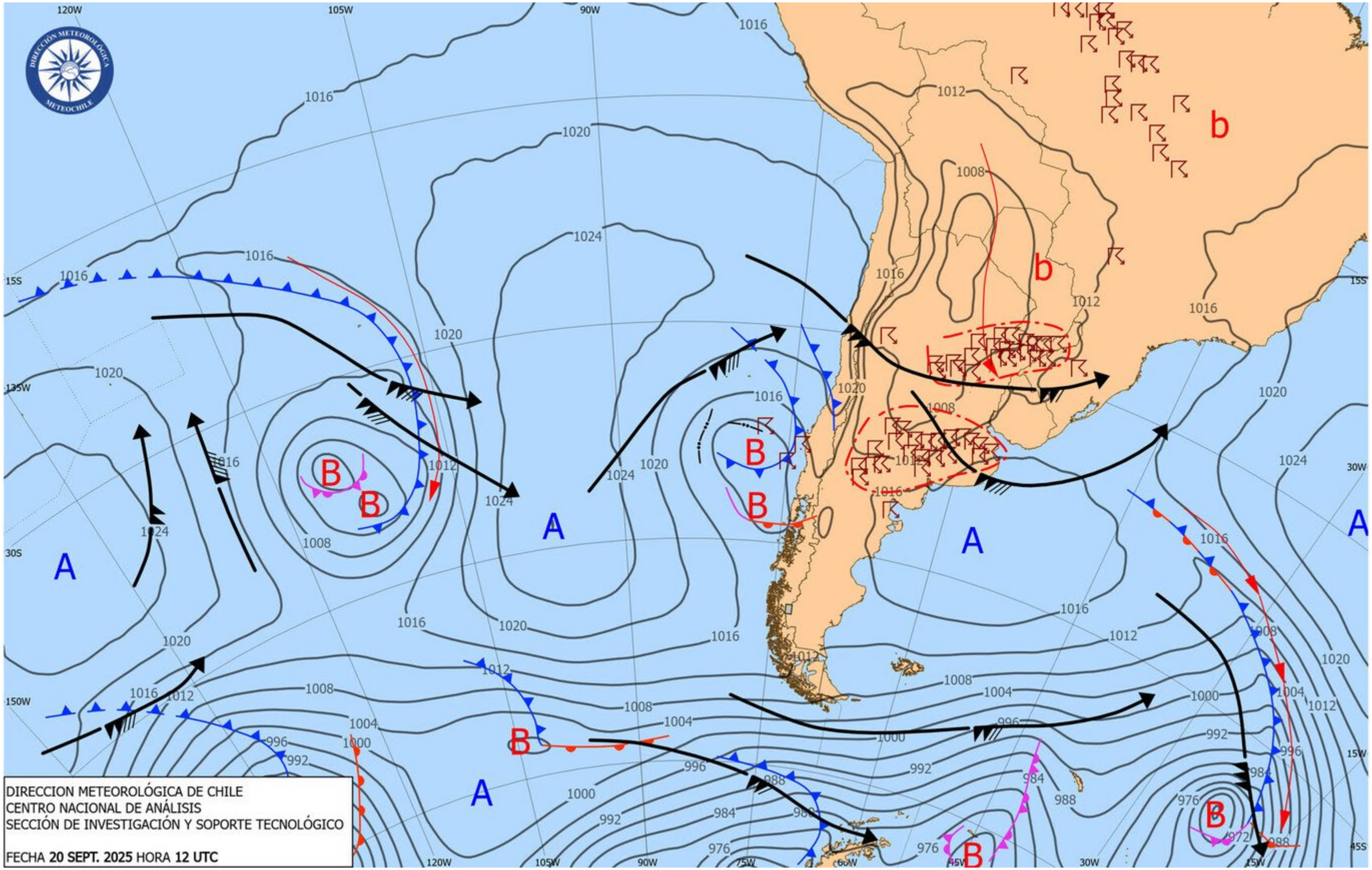
DIRECCION METEOROLÓGICA DE CHILE
CENTRO NACIONAL DE ANÁLISIS
SECCIÓN DE INVESTIGACIÓN Y SOPORTE TECNOLÓGICO
FECHA 20 SEPT. 2025 HORA 12 UTC

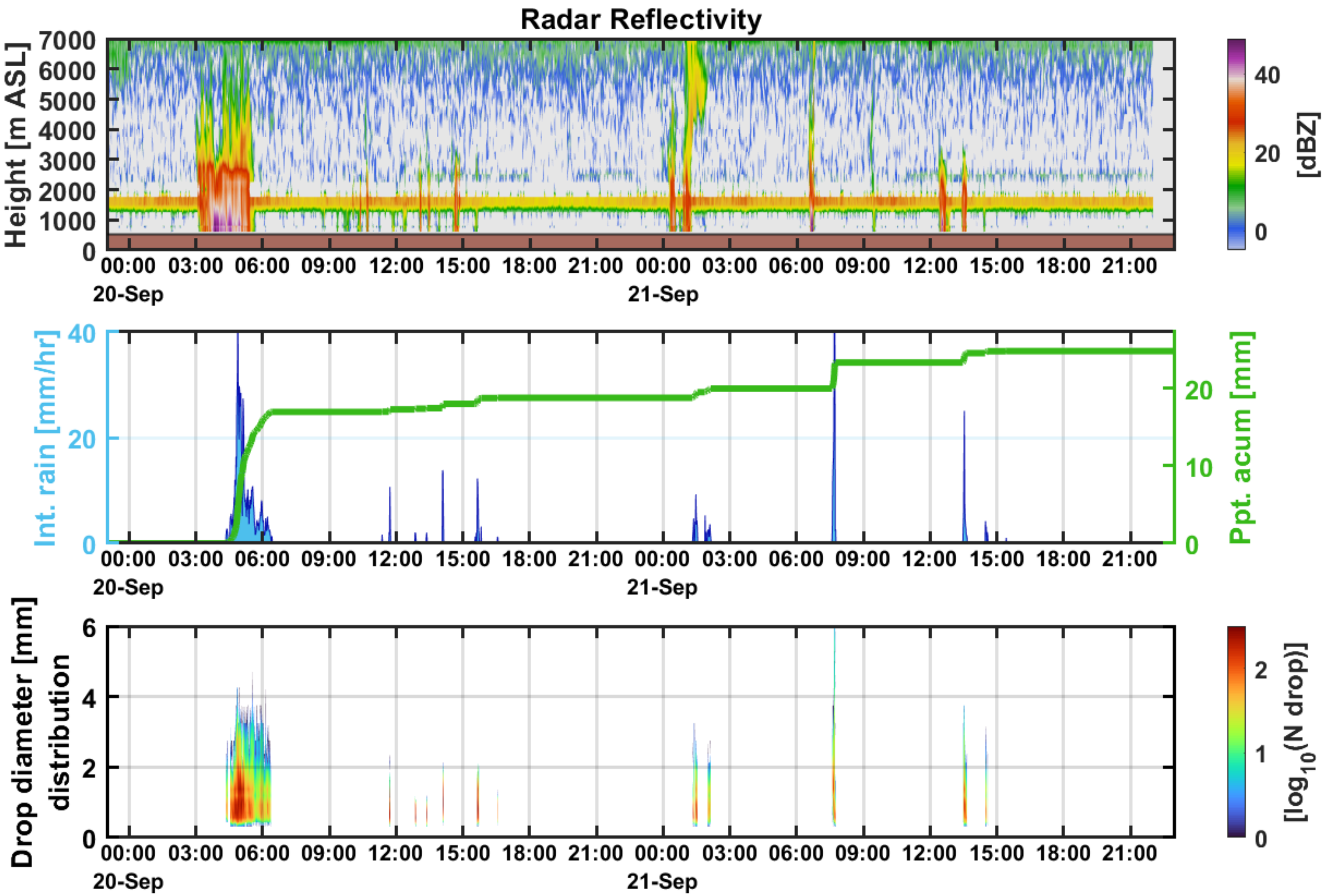

Radar Reflectivity
Height [m ASL]
7000
6000
5000
4000
3000
2000
1000
0
00:00
03:00
06:00
09:00
12:00
15:00
18:00
21:00
00:00
03:00
06:00
09:00
12:00
15:00
18:00
21:00
20-Sep
21-Sep
40
20
0
[dBZ]
Int. rain [mm/hr]
40
20
0
Ppt. acum [mm]
20
10
0
Drop diameter [mm] distribution
6
4
2
0
[log10(N drop)]
2
1
0

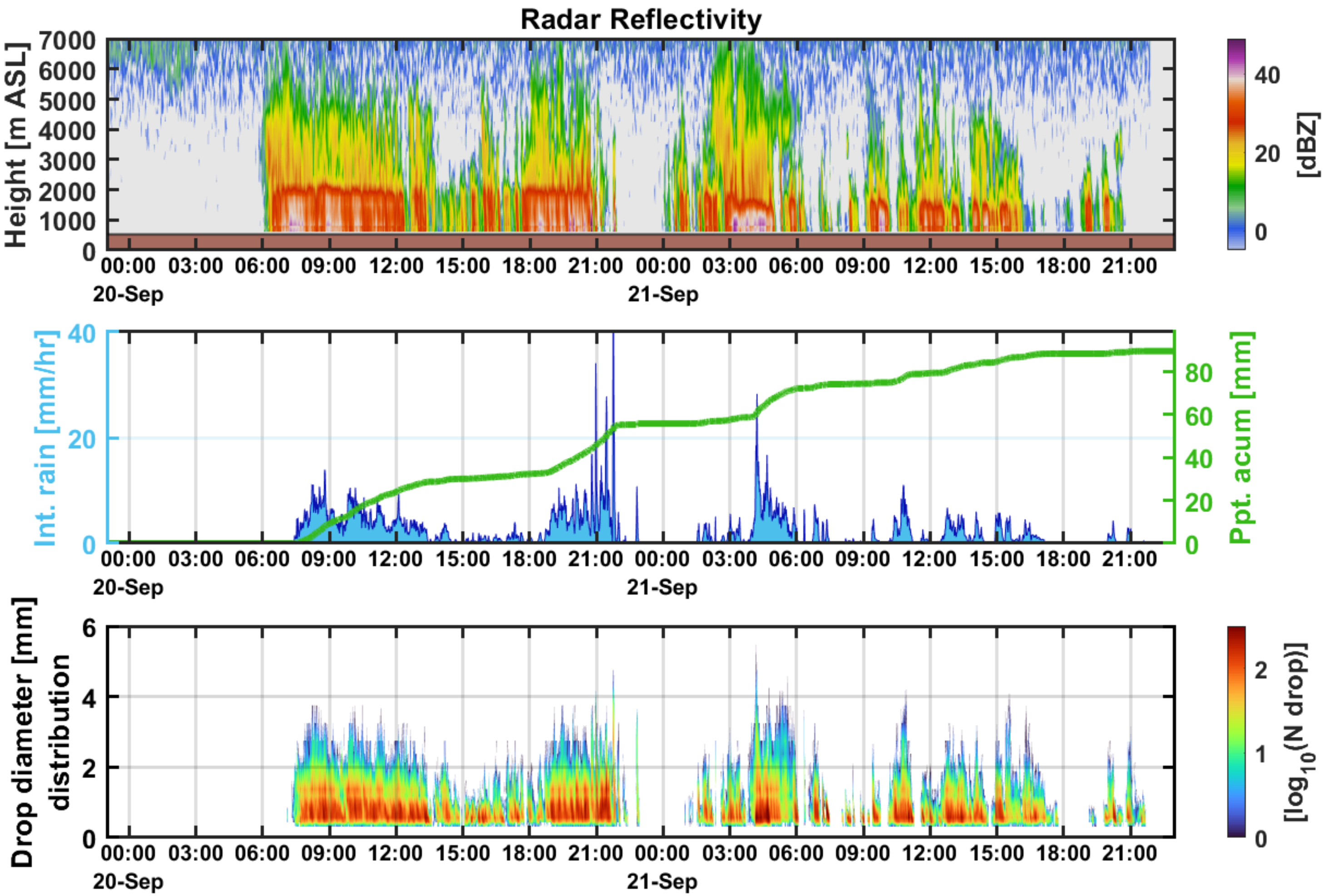
Radar Reflectivity
Height [m ASL]
7000
6000
5000
4000
3000
2000
1000
0
00:00 03:00 06:00 09:00 12:00 15:00 18:00 21:00 00:00 03:00 06:00 09:00 12:00 15:00 18:00 21:00
20-Sep
21-Sep
40
20
0
[dBZ]
Int. rain [mm/hr]
40
20
0
Ppt. acum [mm]
80
60
40
20
0
Drop diameter [mm] distribution
6
4
2
0
2
1
0
[log10(N drop)]

Que hace una tormenta mas jugosa que otra?

El ascenso forzado (wT) sobre la cordillera incrementa el ascenso de gran escala y en consecuencia la precipitación. wT depende a la vez del flujo contra la montaña (U en nuestro caso). Pero no olvidar la humedad!

r[P*,U(z)]

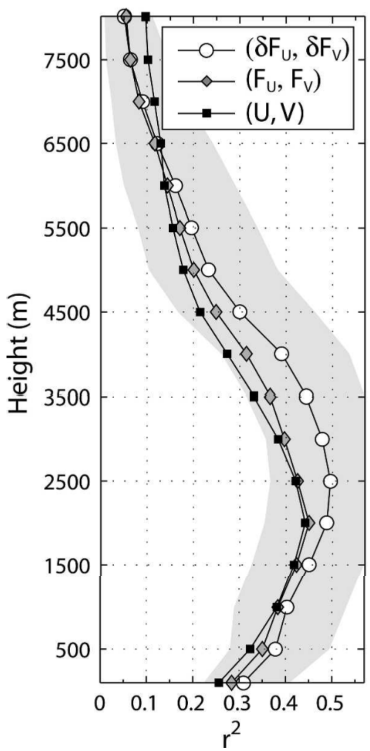


r[P,U(2500 m)]

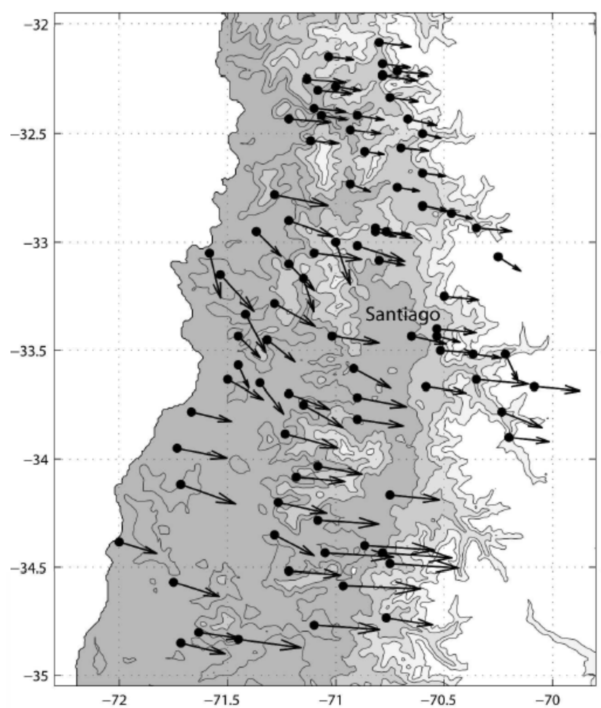


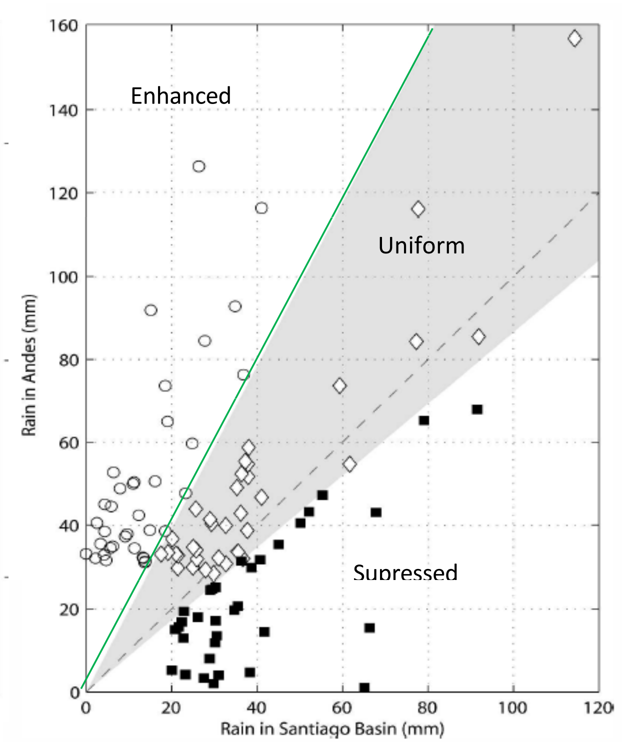


Falvey and Garreaud 2007

**Garreaud et al. 2013**. Using PRECIS-ERA40 data, they show that strong (local) correlation between 850 hPa zonal wind and precipitation extends along south-central Chile because of the orographic enhancement in the windward side of the Andes